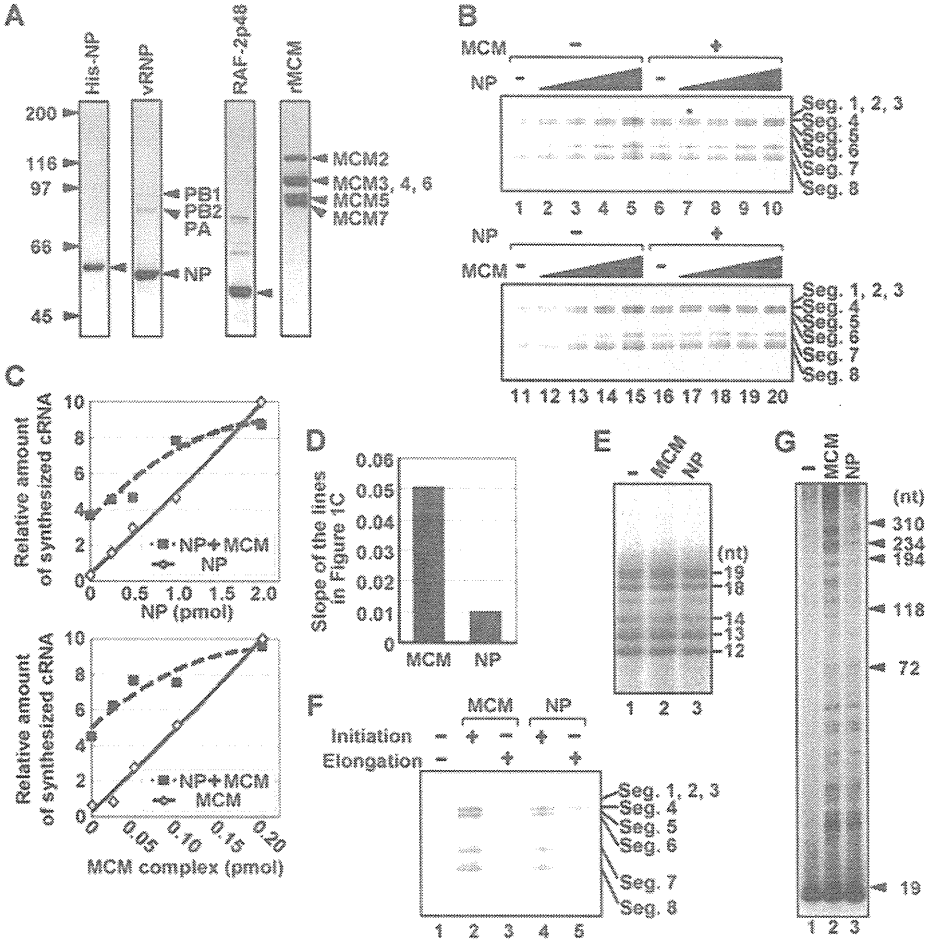

FIG. 1. NP and MCM additively stimulate virus genome replication. (A) Purified recombinant proteins and vRNP. Purified His-NP, vRNP, RAF-2p48/UAP56, and MCM complexes were separated by 7.5% SDS-PAGE and visualized by staining with Coomassie brilliant blue. (B) Stimulatory activity of NP and MCM in cell-free virus genome replication. RNA synthesis was carried out in the absence (lanes 1 to 5) or presence (lanes 6 to 10) of recombinant MCM complex (0.05 pmol of MCM complex) with 0 (lanes 1 and 6), 0.25 (lanes 2 and 7), 0.5 (lanes 3 and 8), 1.0 (lanes 4 and 9), and 2.0 pmol (lanes 5 and 10) of recombinant NP (upper panel). For the experiments shown in the lower panel, we performed the RNA synthesis assay in the absence (lanes 11 to 15) or presence (lanes 16 to 20) of recombinant NP (0.50 pmol) with 0 (lanes 11 and 16), 0.025 (lanes 12 and 17), 0.05 (lanes 13 and 18), 0.10 (lanes 14 and 19), and 0.20 pmol (lanes 15 and 20) of MCM complex (lower panel). (C) Quantitative summary of panel A. The amounts of newly synthesized cRNA corresponding to segment 7 were determined by the ImageJ software. (D) Stimulatory activity per molecule of MCM and NP. The slopes of the lines in the presence of NP or MCM in panel C were determined. (E) Limited elongation assays. Unprimed limited elongation assays were carried out in the absence (lane 1) or presence (lane 2; 0.5 pmol) of MCM or NP (lane 3; 3.0 pmol). (F) NP functions during transition from initiation to elongation reaction. Unprimed limited elongation reactions were performed without (lanes 1, 3, and 5) or with (lanes 2 and 4) either MCM (lane 2; 0.5 pmol) or NP (lane 4; 3.0 pmol). After incubation for 1 h, elongation reactions were restarted by the addition of UTP. For lanes 3 and 5, MCM (0.5 pmol) and NP (3.0 pmol) were added at the restart of elongation reaction, respectively. (G) MCM stimulates the elongation process more effectively than NP. RNA synthesis was carried out in the absence (lane 1) or presence of either MCM (lane 2; 0.5 pmol) or NP (lane 3; 3.0 pmol) with 0.3 μM UTP, 250 μM each ATP, CTP, and GTP, and 10 μCi of [α-^{32}P]UTP (3,000 Ci/mmol). The purified products were separated through 4 to 15% linear gradient PAGE containing 8 M urea and visualized by autoradiography.

nant NP (data not shown). We used as the enzyme source the vRNP containing authentic NP that is bound to the template RNA. Thus, it is quite likely that RNA-free NP but not template-bound NP is required for *de novo* virus genome replication. The RNA synthesis level varied among segments, as previously described (9). For instance, segments 1, 2, and 3 were hardly replicated compared with replication of other segments. The reason for this variation in cRNA synthesis is presently unknown.

NP facilitates the promoter escape of the viral RNA polymerase. Previously, we demonstrated that MCM does not enhance the frequency of replication initiation, but rather makes a nonproductive viral polymerase override the step for abortive synthesis. To examine whether NP is involved in the initiation reaction of virus genome synthesis, we carried out a limited elongation assay, in which UTP is omitted from the reaction mixture and the RNA polymerase pauses at the first adenine residue on the template. The expected lengths of limited elon-

gation products are 12 nt for segments 1, 3, and 7, 13 nt for segments 5 and 8, 14 nt for segment 6, 18 nt for segment 4, and 19 nt for segment 2. Since we detected comparable amounts of each RNA product in the absence or presence of exogenous NP (Fig. 1E), it is concluded that NP, like MCM, does not stimulate the initiation reaction (9). Thus, NP may be required for a step(s) after the initiation and the early elongation steps, in which short cRNAs are synthesized.

To examine whether NP stimulates the transition of the viral polymerase from initiation to elongation, that is, the promoter escape of the viral polymerase, unprimed limited elongation assays were first performed in the absence of UTP, and elongation reactions were restarted by the addition of UTP (Fig. 1F). MCM (0.5 pmol) or exogenous NP (3 pmol) was also added either before or after the limited elongation. The full-length cRNA was synthesized by restarting the limited elongation reaction performed in the presence of MCM (lane 2) or exogenous NP (lane 4) during the limited elongation reaction. Thus, it is quite likely that, to avoid abortive RNA synthesis by the viral polymerase, MCM and NP are required for the viral polymerase prior to its movement along a 12- to 19-nt-long vRNA template from the 3′ terminus of vRNA, where the hairpin loop and double-stranded promoter region are located. Since the initiation reaction was not stimulated by NP (Fig. 1E) and since the viral polymerase could not transit from initiation to elongation in the absence of NP (Fig. 1F), it is possible that NP stimulates elongation complexes during the promoter escape of the viral polymerase, as does MCM (9). A cell-free virus genome replication reaction was also carried out (Fig. 1G) in the presence of MCM (lane 2; 0.5 pmol) or NP (lane 3; 3 pmol) with a low concentration of UTP to slow down the reaction and synthesize a ladder of nascent cRNA chains in order to examine the length of elongated nascent cRNA chains. We found that comparable amounts of cRNA with a shorter length (~100 nt) are synthesized in the presence of either MCM or NP. In contrast, the amount of longer cRNAs (>100 nt) stimulated by MCM was greater than that stimulated by NP (Fig. 1G, compare lane 2 with lane 3). Therefore, it is quite likely that MCM promotes the elongation process more effectively than NP, possibly due to the weak interaction of exogenously added NP with long nascent cRNA, as described later. Taking these results together, it is strongly suggested that NP, like MCM, stimulates the promoter escape of the viral polymerase. Previous reports showed that the target of MCM is PA (9), whereas that of NP is PB1 and PB2 (1). Therefore, it is possible that the replication stimulation mechanisms of NP and MCM are distinct from each other.

Encapsidation of newly synthesized virus genome by NP. Previously, we proposed that MCM stimulates virus genome replication by acting as a scaffold between nascent cRNA chains and the viral polymerase during the promoter escape of the polymerase (9). Since NP has both RNA and viral polymerase binding activities, it should be speculated that NP, like MCM, also functions as a scaffold between newly synthesized RNA and the viral polymerase. To address this, we tried to pull down the replicated cRNA chains associated with His-tagged MCM or NP using Ni-nitrilotriacetic acid (NTA) resin (Fig. 2A). The cell-free virus genome replication reaction was carried out in the presence of an equal molar amount of MCM (lanes 1 and 3) or NP (lanes 2 and 4) with a low concentration

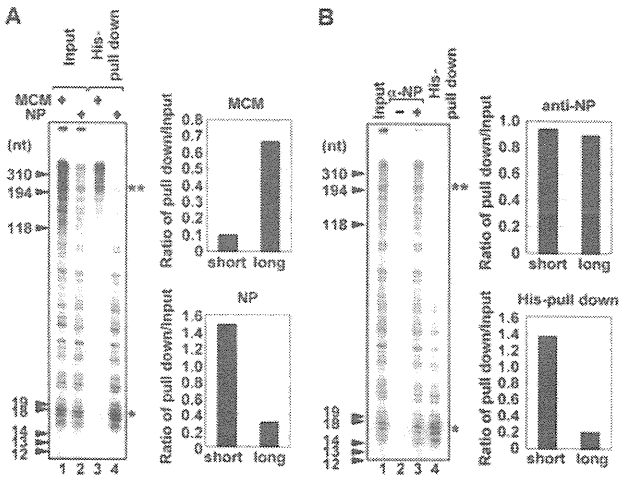

FIG. 2. Encapsidation of nascent cRNA with NP. (A) *De novo* RNA synthesis was carried out in the presence of His-MCM (lanes 1 and 3; 20 pmol) or His-NP (lanes 2 and 4; 20 pmol) with 0.3 μM UTP and 250 μM each ATP, CTP, and GTP and 10 μCi of [α-^{32}P]UTP (3,000 Ci/mmol) in a final volume of 200 μl. The products were purified with His-MCM (lane 3) or His-NP (lane 4) by using Ni-NTA resin. Lanes 1 and 2 represent 20% of the input amounts. The band intensities of short (*) and long (**) nascent cRNA products were quantitatively measured with ImageJ software, and the relative intensity of newly synthesized cRNA coprecipitated with MCM or NP against the input fraction is indicated. (B) *De novo* RNA synthesis was carried out with the authentic vRNP in the presence of His-NP as described for panel A. The newly synthesized RNA products were coimmunoprecipitated without (lane 2) or with (lane 3) anti-NP antibody. Lane 1 shows 20% of the input amount. The product purified by Ni-NTA resin is also represented in lane 4. The band intensities of short (*) and long (**) nascent cRNA products were quantitatively measured with ImageJ software, and the relative intensity of newly synthesized cRNA precipitated by using anti-NP antibody or Ni-NTA resin against input fraction is indicated. α, anti.

of UTP in order to examine the length of copurified RNA as shown in Fig. 1G. As shown in input lanes, MCM stimulated the elongation process more effectively than NP (Fig. 1E and 2A, lanes 1 and 2). Further, longer nascent cRNA chains were preferentially copurified with MCM (Fig. 2A, lane 3), suggesting that MCM stabilizes the elongation complex and thereby makes the viral polymerase escape the promoter successfully. It also seems likely that MCM has a role in the elongation process, but its precise mechanism is still unknown. In contrast, rather shorter cRNA chains were associated with exogenous NP (lane 4). After or along with virus genome replication, the newly synthesized virus genome has to be encapsidated by exogenous NP to form RNP complexes as templates for the next phase of virus genome replication and to protect the virus genome from degradation by cellular nucleases (33). It is hypothesized that encapsidation proceeds by targeting exogenous NP to the nascent RNA through the interaction between NP and the viral polymerase bound to the 5′ end of the nascent RNA to allow NP to interact with the viral RNA preferentially with respect to other cellular RNA species (1, 8, 11, 22), and then subsequently NP is recruited through NP-NP oligomerization (3, 23). In our cell-free system, we found that exogenous NP interacts with shorter cRNA (Fig. 2A, lane 4) without the addition of soluble viral polymerases, which could bind to

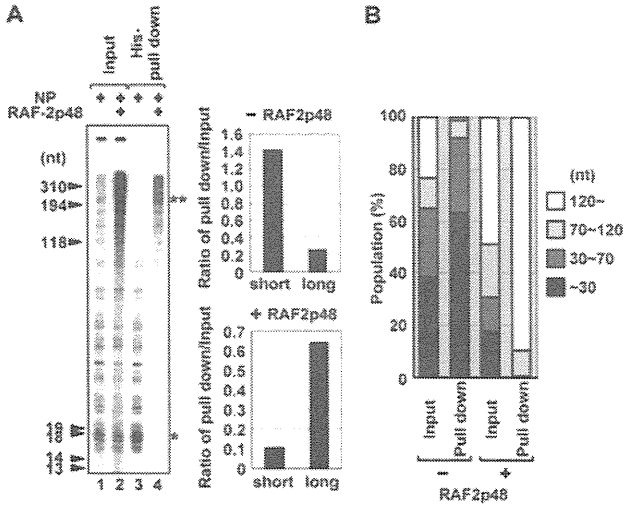

FIG. 3. The stimulatory activity of RAF-2p48/UAP56 in encapsidation of nascent cRNA. (A) RNA synthesis was performed in the absence (lanes 1 and 3) or presence (lanes 2 and 4) of recombinant RAF-2p48/UAP56 with His-NP as described in the legend of Fig. 2. The products were purified with His-NP by using Ni-NTA resin (lanes 3 and 4). Twenty percent of the input amounts is shown in lanes 1 and 2. The band intensities of short (*) and long (**) nascent cRNA products were quantitatively measured with ImageJ software, and the relative intensity of cRNA coprecipitated with NP in the absence or presence of RAF-2p48 against input fraction is indicated. (B) The band intensities of the regions corresponding to RNAs of less than 30 nt, 30 to 70 nt, 70 to 120 nt, and more than 120 nt in each lane in panel A were quantitatively measured with ImageJ software, and the results are indicated as a percentage of the total intensity of each lane.

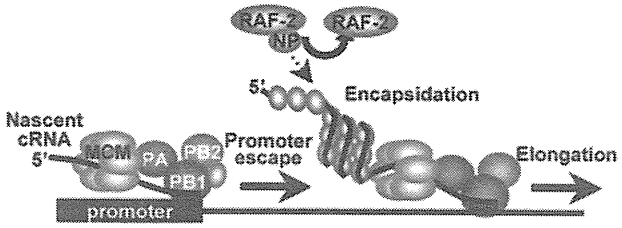

FIG. 4. Proposed model. NP facilitates the promoter escaping from the viral polymerase through the interaction between NP and the viral polymerase in an RNA binding activity-independent manner. During elongation step, RAF-2p48/UAP56 stimulates the coreplicational encapsidation of newly synthesized cRNA with exoge
increasing the processivity of the viral polymerase.

the 5′ end of the nascent RNA and be a target of NP. It might be explained that the primary targeting of NP to the nascent RNA easily occurs since there is no RNA target other than the nascent RNA in our system. However, it is worth noting that encapsidation of longer nascent cRNA by NP was not achieved when NP was simply added to the system (lane 4). This raises a question of how the newly synthesized virus genome is encapsidated with NP free of RNA.

NP recognizes the phosphodiester backbone of ssRNA in a specific sequence-independent manner. We used, as the enzyme source, the vRNP containing authentic NP, which is bound to the template RNA. Thus, it is reasonably hypothesized that newly synthesized cRNA chains remain associated with the template RNP, possibly by partial hybridization of the nascent cRNA with template vRNA and/or the interaction of nascent cRNA with template-bound authentic NP instead of exogenous NP. To address this, we immunopurified the template-bound authentic NP of vRNP in the presence of exogenous His-NP using anti-NP antibody (Fig. 2B). The length of RNA products associated with authentic NP or both authentic NP and exogenous His-NP (lane 3) was clearly distinct from that of RNA products interacting with only exogenous His-NP (lane 4). From these results, it is assumed that the nascent cRNA product is hardly encapsidated with exogenous NP since the nascent cRNA tends to interact more with template-bound NP than exogenous NP and might partially hybridize with the template.

Encapsidation with NP mediated by RAF-2p48/UAP56. As shown in Fig. 2, it is assumed that some factor(s) may be missing in the encapsidation of nascent cRNA products with exogenous NP. Previously, RAF-2p48/UAP56/BAT1 (here, designated RAF-2p48/UAP56) belonging to the DExD-box family of ATP-dependent RNA helicase (13), also reported as NPI-5 (20), was identified as a host factor that binds to NP and stimulates influenza virus RNA synthesis from exogenously added model vRNA templates (16) and that is involved in splicing of cellular pre-mRNAs and messenger RNP maturation of cellular and viral transcripts (4, 25, 29). RAF-2p48/UAP56 binds to NP free of RNA but not to an NP-RNA complex and facilitates NP-RNA complex formation as a molecular chaperone for NP. Therefore, it was proposed that RAF-2p48/UAP56 is involved in the arrangement of NP on the template. However, its precise roles, including the requirement for the encapsidation process, have not yet been uncovered. Thus, we tried to examine whether RAF-2p48/UAP56 facilitates the encapsidation of newly synthesized RNA with exogenous NP (Fig. 3A). We found that long nascent cRNA was encapsidated with exogenous NP by the addition of RAF-2p48/UAP56 (Fig. 3A, compare lane 4, in which RAF-2p48/UAP56 is present, with lane 3, in which RAF-2p48/UAP56 is absent). The ATP-dependent RNA unwinding activity of RAF-2p48/UAP56 was not required for the encapsidation of nascent chains since the encapsidation occurred in the presence of ATPγS, which is a nonhydrolyzable analog of ATP (data not shown). Therefore, we propose a model whereby RAF-2p48/UAP56 facilitates the formation of RNP complexes by coreplicationally transferring exogenous NP to the nascent cRNA chain. It is unlikely that RAF-2p48/UAP56 remodels secondary structures of template and newly synthesized cRNA by its potential RNA helicase activity (Fig. 4). Furthermore, RAF-2p48/UAP56 stimulated the elongation activity of the viral polymerase, possibly by facilitating the encapsidation of nascent cRNA (Fig. 3, lane 2). It is speculated that the coreplicational encapsidation of nascent cRNA by NP may prevent the premature termination of RNA synthesis by avoiding a secondary structure of nascent RNA, which is hypothesized to be one of the causative factors in the termination process of other RNA polymerases (10, 27). Therefore, it is possible that the encapsidation of the nascent RNA with exogenous NP mediated by RAF-2p48/UAP56 increases the processivity of the

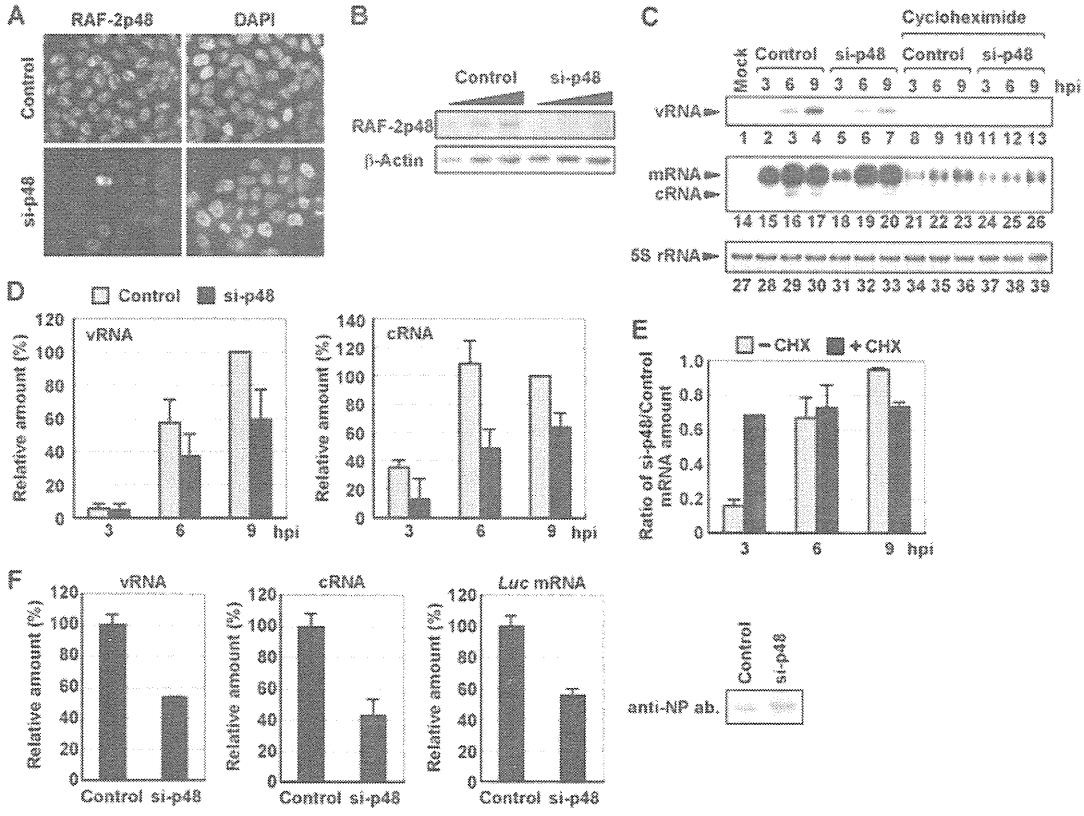

FIG. 5. Involvement of RAF-2p48/UAP56 in influenza virus genome replication in infected cells. (A) At 48 h posttransfection, cells transfected with either a control or siRNA against the RAF-2p48/UAP56 ORF (si-p48) were subjected to indirect immunofluorescence assay with anti-RAF-2p48/UAP56 antibody. Nuclear DNA stained with 4′,6-diamidino-2-phenylindole (DAPI) is also shown. Images were acquired under the same exposure time by a fluorescence microscope system (Axiovision; Carl Zeiss). (B) Expression level of RAF-2p48/UAP56. The lysates prepared from control and RAF-2p48/UAP56 knockdown cells (5×10^3, 1×10^4, and 2×10^4 cells) were separated by SDS-PAGE and then visualized by Western blotting assays with anti-NP and β-actin antibodies. (C, D, and E) Level of viral RNAs in infected RAF-2p48/UAP56 knockdown cells. Control and RAF-2p48/UAP56 knockdown cells were infected with influenza virus in the absence (lanes 1 to 7 and 14 to 20) or presence of cycloheximide (lanes 7 to 13 and 21 to 26) for 0, 3, 6, and 9 h. Primer extension assays were carried out with primers specific for segment 5 vRNA or m/cRNA as described in Materials and Methods. As a loading control, 5S rRNA was also detected (lanes 27 to 39). The band intensities were quantitatively measured by ImageJ software, and the results of three independent experiments are summarized in panel D and are indicated in panel E as the ratio of the mRNA amount in RAF-2p48/UAP56 knockdown cells to that in control cells with or without CHX. (F) The level of viral RNAs synthesized from a reconstituted model replicon in RAF-2p48/UAP56 knockdown cells. Control and RAF-2p48/UAP56 knockdown cells were transfected with plasmids expressing PB1, PB2, PA, and NP and model vRNA encoding the luciferase gene as described in Materials and Methods. At 12 h posttransfection, total RNAs were purified and then subjected to reverse transcription, followed by quantitative real-time PCR with primer sets specific for vRNA, cRNA, and luciferase mRNA. The expression level of NP protein in control and RAF-2p48/UAP56 knockdown cells was also detected by a Western blotting assay with anti-NP antibody (ab).

viral polymerase by avoiding inappropriate secondary structures of nascent cRNA.

Involvement of RAF-2p48/UAP56 in influenza virus genome replication in infected cells. Finally, we tried to examine whether RAF-2p48/UAP56 functions in influenza virus genome replication in cultured cells using siRNA-mediated gene silencing. At 48 h posttransfection of siRNA corresponding to the RAF-2p48/UAP56 ORF, the expression level of RAF-2p48/UAP56 in knockdown cells decreased to approximately 30% of that of cells transfected with the nontargeting siRNA used as a negative control (Fig. 5A and B). We carried out quantitative primer extension assays with appropriate primers specific for each vRNA and mRNA/cRNA of segment 5 (Fig. 5C and D). We confirmed that the product corresponding to cRNA was not found from a fraction bound with oligo(dT) cellulose (data not shown). This result showed that the accumulation of vRNA and cRNA was reduced and delayed in RAF-2p48/UAP56 knockdown cells compared with levels in control cells (Fig. 5C, lanes 1 to 7 and 14 to 20, and D). The same results were obtained for other segments (data not shown). It is proposed that nascent cRNA is degraded unless it is encapsidated with viral RNA polymerase and NP (33). In addition, the results shown in Fig. 3 and a previous report (16) demonstrated that RAF-2p48/UAP56 stimulates the viral polymerase activity. Thus, RAF-2p48/UAP56 might be involved in virus genome replication and encapsidation in infected cells. We also found that the level of NP mRNA in RAF-2p48/UAP56 knockdown cells decreased to 15% in control cells at 3 hpi (Fig. 5C, lanes 15 and 18, and E). In contrast, comparable amounts of NP mRNA were found in both control and RAF-

2p48/UAP56 knockdown cells at 6 and 9 hpi (Fig. 5C, lanes 16, 17, 19, and 20) since the amount of vRNA template sufficient for viral mRNA synthesis might be accumulated at 6 and 9 hpi, but the replication activity was reduced and delayed in RAF-2p48/UAP56 knockdown cells. To confirm the effect of RAF-2p48/UAP56 on viral transcription, we utilized cycloheximide (CHX), a potent protein synthesis inhibitor (Fig. 5C, lanes 8 to 13 and 21 to 26, and E). A previous report showed that CHX suppresses viral protein synthesis and thereby leads to degradation of replicated viral RNA but not mRNA since new vRNP formation was repressed (33). Therefore, we could examine the amount of viral mRNA synthesized from incoming vRNP independent of the level of vRNA accumulation in the presence of CHX (Fig. 5C, lanes 8 to 13, and E). The level of NP mRNA in RAF-2p48/UAP56 knockdown cells was reduced to 70% in control cells in the presence of CHX at 3 hpi (Fig. 5C, lanes 21 and 24, and E). Therefore, it is likely that the reduction of viral mRNA synthesis in RAF-2p48/UAP56 knockdown cells is mainly due to the decrease of vRNP accumulation in the absence of CHX although RAF-2p48/UAP56 has a stimulatory role in viral transcription, possibly by arrangement of NP on template and/or the nuclear export-competent messenger RNP formation (25). To rule out the possibility that the reduction of vRNA and cRNA synthesis was caused by the reduction of viral protein synthesis, we carried out a viral model replicon assay (19, 30) in which active vRNP complexes were reconstituted with PB1, PB2, PA, and NP and the model vRNA encoding the luciferase gene, as described in Materials and Methods (Fig. 5F). With this system, we could examine the viral polymerase activity independent of the expression level of viral proteins since viral proteins were expressed from plasmids under the control of cellular RNA polymerase II promoter in this assay. Results shown in Fig. 5F indicate that vRNA, cRNA, and viral mRNA synthesis was decreased in RAF-2p48/UAP56 knockdown cells compared with that in control cells even in the presence of comparable amounts of NP in both cells. We found that NP synthesized in RAF-2p48/UAP56 knockdown cells migrates differently from that in control cells (Fig. 5F). Previous reports showed that NP is modified by phosphorylation (23) and that its N-terminal region is digested by caspase (35), but the involvement of RAF-2p48/UAP56 in these is not known at present.

It is well known that NP is one of proteins responsible for virus genome replication (15, 18, 27, 33). Recently, it is reported that ubiquitination of NP regulates virus genome replication (12). It is proposed that the soluble viral polymerase might act as a replicative enzyme in *trans*, but transcription occurs from template-bound viral polymerase in *cis* (8). In this study and recent reports (9, 31–33), *de novo* cRNA synthesis is found from template-bound viral polymerase; thus, it could be explained that the soluble viral polymerase might have stimulatory activity but is not completely essential for the synthesis of nascent cRNA. The viral nuclear export protein (NEP/NS2) is also involved in the accumulation level of vRNA and cRNA (26). Further, it is reported that small noncoding RNAs derived from the influenza virus genome might regulate viral transcription and replication through their interaction with viral polymerase complexes (21). To further understand the mechanism of influenza viral genome replication, precise analyses of a functional replicative enzyme including viral and cellular factors are required.

ACKNOWLEDGMENTS

We thank Y. Ishimi (Ibaraki University) for the generous gifts of baculoviruses expressing MCM proteins. This research was supported in part by a grant-in-aid from the Ministry of Education, Culture, Sports, Science, and Technology of Japan (to K.N. and F.M.) and Research Fellowships of the Japanese Society for the Promotion of Science (to A.K.).

REFERENCES

1. **Biswas, S. K., P. L. Boutz, and D. P. Nayak.** 1998. Influenza virus nucleoprotein interacts with influenza virus polymerase proteins. J. Virol. **72:**5493–5501.
2. **Blumberg, B. M., M. Leppert, and D. Kolakofsky.** 1981. Interaction of VSV leader RNA and nucleocapsid protein may control VSV genome replication. Cell **23:**837–845.
3. **Chan, W. H., et al.** 2010. Functional analysis of the influenza virus H5N1 nucleoprotein tail loop reveals amino acids that are crucial for oligomerization and ribonucleoprotein activities. J. Virol. **84:**7337–7345.
4. **Fleckner, J., M. Zhang, J. Valcarcel, and M. R. Green.** 1997. U2AF65 recruits a novel human DEAD box protein required for the U2 snRNP-branchpoint interaction. Genes Dev. **11:**1864–1872.
5. **Honda, A., et al.** 1990. Purification and molecular structure of RNA polymerase from influenza virus A/PR8. J. Biochem. **107:**624–628.
6. **Honda, A., K. Ueda, K. Nagata, and A. Ishihama.** 1988. RNA polymerase of influenza virus: role of NP in RNA chain elongation. J. Biochem. **104:**1021–1026.
7. **Horikami, S. M., J. Curran, D. Kolakofsky, and S. A. Moyer.** 1992. Complexes of Sendai virus NP-P and P-L proteins are required for defective interfering particle genome replication in vitro. J. Virol. **66:**4901–4908.
8. **Jorba, N., R. Coloma, and J. Ortin.** 2009. Genetic trans-complementation establishes a new model for influenza virus RNA transcription and replication. PLoS Pathog. **5:**e1000462.
9. **Kawaguchi, A., and K. Nagata.** 2007. De novo replication of the influenza virus RNA genome is regulated by DNA replicative helicase, MCM. EMBO J. **26:**4566–4575.
10. **Komissarova, N., J. Becker, S. Solter, M. Kireeva, and M. Kashlev.** 2002. Shortening of RNA:DNA hybrid in the elongation complex of RNA polymerase is a prerequisite for transcription termination. Mol. Cell **10:**1151–1162.
11. **Labadie, K., E. Dos Santos Afonso, M. A. Rameix-Welti, S. van der Werf, and N. Naffakh.** 2007. Host-range determinants on the PB2 protein of influenza A viruses control the interaction between the viral polymerase and nucleoprotein in human cells. Virology **362:**271–282.
12. **Liao, T. L., C. Y. Wu, W. C. Su, K. S. Jeng, and M. M. Lai.** 2010. Ubiquitination and deubiquitination of NP protein regulates influenza A virus RNA replication. EMBO J. **29:**3879–3890.
13. **Linder, P., and F. Stutz.** 2001. mRNA export: travelling with DEAD box proteins. Curr. Biol. **11:**R961–R963.
14. **Masters, P. S., and A. K. Banerjee.** 1988. Complex formation with vesicular stomatitis virus phosphoprotein NS prevents binding of nucleocapsid protein N to nonspecific RNA. J. Virol. **62:**2658–2664.
15. **Medcalf, L., E. Poole, D. Elton, and P. Digard.** 1999. Temperature-sensitive lesions in two influenza A viruses defective for replicative transcription disrupt RNA binding by the nucleoprotein. J. Virol. **73:**7349–7356.
16. **Momose, F., et al.** 2001. Cellular splicing factor RAF-2p48/NPI-5/BAT1/UAP56 interacts with the influenza virus nucleoprotein and enhances viral RNA synthesis. J. Virol. **75:**1899–1908.
17. **Nagata, K., A. Kawaguchi, and T. Naito.** 2008. Host factors for replication and transcription of the influenza virus genome. Rev. Med. Virol. **18:**247–260.
18. **Newcomb, L. L., et al.** 2009. Interaction of the influenza a virus nucleocapsid protein with the viral RNA polymerase potentiates unprimed viral RNA replication. J. Virol. **83:**29–36.
19. **Obayashi, E., et al.** 2008. The structural basis for an essential subunit interaction in influenza virus RNA polymerase. Nature **454:**1127–1131.
20. **Palese, P., P. Wang, T. Wolff, and R. E. O'Neill.** 1997. Host-viral protein-protein interactions in influenza virus replication, p. 327–340. *In* M. A. McCrae (ed.), Molecular aspects of host-pathogen interaction. Cambridge University Press, Cambridge, United Kingdom.
21. **Perez, J. T., et al.** 2010. Influenza A virus-generated small RNAs regulate the switch from transcription to replication. Proc. Natl. Acad. Sci. U. S. A. **107:**11525–11530.
22. **Poole, E., D. Elton, L. Medcalf, and P. Digard.** 2004. Functional domains of the influenza A virus PB2 protein: identification of NP- and PB1-binding sites. Virology **321:**120–133.
23. **Portela, A., and P. Digard.** 2002. The influenza virus nucleoprotein: a multifunctional RNA-binding protein pivotal to virus replication. J. Gen. Virol. **83:**723–734.

24. **Qanungo, K. R., D. Shaji, M. Mathur, and A. K. Banerjee.** 2004. Two RNA polymerase complexes from vesicular stomatitis virus-infected cells that carry out transcription and replication of genome RNA. Proc. Natl. Acad. Sci. U. S. A. **101:**5952–5957.
25. **Read, E. K., and P. Digard.** 2010. Individual influenza A virus mRNAs show differential dependence on cellular NXF1/TAP for their nuclear export. J. Gen. Virol. **91:**1290–1301.
26. **Robb, N. C., M. Smith, F. T. Vreede, and E. Fodor.** 2009. NS2/NEP protein regulates transcription and replication of the influenza virus RNA genome. J. Gen. Virol. **90:**1398–1407.
27. **Shapiro, G. I., and R. M. Krug.** 1988. Influenza virus RNA replication in vitro: synthesis of viral template RNAs and virion RNAs in the absence of an added primer. J. Virol. **62:**2285–2290.
28. **Shimizu, K., H. Handa, S. Nakada, and K. Nagata.** 1994. Regulation of influenza virus RNA polymerase activity by cellular and viral factors. Nucleic Acids Res. **22:**5047–5053.
29. **Strasser, K., et al.** 2002. TREX is a conserved complex coupling transcription with messenger RNA export. Nature **417:**304–308.
30. **Sugiyama, K., et al.** 2009. Structural insight into the essential PB1-PB2 subunit contact of the influenza virus RNA polymerase. EMBO J. **28:**1803–1811.
31. **Vreede, F. T., and G. G. Brownlee.** 2007. Influenza virion-derived viral ribonucleoproteins synthesize both mRNA and cRNA in vitro. J. Virol. **81:**2196–2204.
32. **Vreede, F. T., H. Gifford, and G. G. Brownlee.** 2008. Role of initiating nucleoside triphosphate concentrations in the regulation of influenza virus replication and transcription. J. Virol. **82:**6902–6910.
33. **Vreede, F. T., T. E. Jung, and G. G. Brownlee.** 2004. Model suggesting that replication of influenza virus is regulated by stabilization of replicative intermediates. J. Virol. **78:**9568–9572.
34. **Yamanaka, K., A. Ishihama, and K. Nagata.** 1990. Reconstitution of influenza virus RNA-nucleoprotein complexes structurally resembling native viral ribonucleoprotein cores. J. Biol. Chem. **265:**11151–11155.
35. **Zhirnov, O. P., T. E. Konakova, W. Garten, and H. Klenk.** 1999. Caspase-dependent N-terminal cleavage of influenza virus nucleocapsid protein in infected cells. J. Virol. **73:**10158–10163.

OPEN ACCESS Freely available online

PLoS one

Tamiflu-Resistant but HA-Mediated Cell-to-Cell Transmission through Apical Membranes of Cell-Associated Influenza Viruses

Kotaro Mori[☯], Takahiro Haruyama[☯¤], Kyosuke Nagata*

Department of Infection Biology, Faculty of Medicine and Graduate School of Comprehensive Human Sciences, University of Tsukuba, Tsukuba, Japan

Abstract

The infection of viruses to a neighboring cell is considered to be beneficial in terms of evasion from host anti-virus defense systems. There are two pathways for viral infection to "*right next door*": one is the virus transmission through cell-cell fusion by forming syncytium without production of progeny virions, and the other is mediated by virions without virus diffusion, generally designated cell-to-cell transmission. Influenza viruses are believed to be transmitted as *cell-free* virus from infected cells to uninfected cells. Here, we demonstrated that influenza virus can utilize cell-to-cell transmission pathway through apical membranes, by handover of virions on the surface of an infected cell to adjacent host cells. Live cell imaging techniques showed that a recombinant influenza virus, in which the *neuraminidase* gene was replaced with the *green fluorescence protein* gene, spreads from an infected cell to adjacent cells forming infected cell clusters. This type of virus spreading requires HA activation by protease treatment. The cell-to-cell transmission was also blocked by amantadine, which inhibits the acidification of endosomes required for uncoating of influenza virus particles in endosomes, indicating that functional hemagglutinin and endosome acidification by M2 ion channel were essential for the cell-to-cell influenza virus transmission. Furthermore, in the cell-to-cell transmission of influenza virus, progeny virions could remain associated with the surface of infected cell even after budding, for the progeny virions to be passed on to adjacent uninfected cells. The evidence that cell-to-cell transmission occurs in influenza virus lead to the caution that local infection proceeds even when treated with neuraminidase inhibitors.

Citation: Mori K, Haruyama T, Nagata K (2011) Tamiflu-Resistant but HA-Mediated Cell-to-Cell Transmission through Apical Membranes of Cell-Associated Influenza Viruses. PLoS ONE 6(11): e28178. doi:10.1371/journal.pone.0028178

Editor: Ron A. M. Fouchier, Erasmus Medical Center, The Netherlands

Received July 8, 2011; **Accepted** November 2, 2011; **Published** November 30, 2011

Funding: This work was supported in part by a grant-in-aid from the Ministry of Education, Culture, Sports, Science, and Technology of Japan (to KN: #20249025). The funders had no role in study design, data collection and analysis, decision to publish, or preparation of the manuscript. The authors received no additional external funding for this study.

Competing Interests: The authors have declared that no competing interests exist.

* E-mail: knagata@md.tsukuba.ac.jp

☯ These authors contributed equally to this work.

¤ Current address: Central Research Center, AVSS Corporation, Nagasaki, Japan

Introduction

It is generally accepted that viruses, released as *cell-free* virions from an infected cell, transmit to distant cells and tissues. This spreading pathway contributes to wide-ranged diffusion of *cell-free* viruses. However, in this spreading pathway, viruses are exposed to host anti-virus defense systems. In contrast, direct infection to a neighboring cell is considered to be beneficial for the virus in terms of evasion from the host anti-virus defense. There are two typical manners in infection to "*right next door*": one is the virus transmission through cell-cell fusion by forming syncytium without production of progeny virions, and the other is mediated by virions without virus diffusion, generally designated cell-to-cell transmission [1,2].

The cell-cell fusion infection pathway is characteristic for a variety of virus such as paramyxoviruses, herpesviruses, some retroviruses, and so on. For example in the case of measles virus belonging to *Paramyxoviridae*, infection is initiated by the interaction of the viral hemagglutinin glycoprotein with host cell surface receptors. The virus penetrates into the cell through membrane fusion mediated by the interaction of the fusion glycoprotein. In later stages of infection, newly synthesized glycoproteins accumulate at the cell membrane resulting in fusion of the infected cell with neighboring cells by producing syncytia. Thus, viruses can spread from cell to cell without producing *cell-free* virus particles.

The examples of the cell-to-cell transmission are diverse, and these mechanisms are dependent on pairs of viruses and host cells. Vaccinia virus particles bound on the filopodium of an infected cell are repelled toward neighboring uninfected cells by the formation of filopodia using actin filament [3]. The filopodia direct viruses to uninfected cells. Immunotropic viruses including retroviruses utilize an immunological synapse, designed as virological synapses for the cell-to-cell transmission [4–7]. Claudin-1 and occludin, components of tight junction, are involved in hepatitis C virus (HCV) entry through the cell-to-cell transmission [8,9]. The cell-to-cell transmission through tight junction is also observed in other viruses which infect epithelial layers [10,11]. These retroviruses and HCV remain on the surface of an infected cell even after budding. The uninfected cells adjacent to these infected cells can accept or take over viruses from

the infected cell. Thus, the cell-to-cell transmission can be categorized into two manners based on the state of infecting viruses, either *cell-free* or cell-associated virions.

Influenza virus, belonging to the family of *Orthomyxoviridae*, is one of the most serious zoonotic pathogens and causes seasonal epidemics or periodic pandemics among human beings around the world. The viral envelope consists of a lipid bilayer derived from cells that anchors three of viral transmembrane proteins, hemagglutinin (HA), neuraminidase (NA), and matrix protein 2 (M2). Influenza virus infection is initiated by the attachment of HA on virus particles to cell surface receptors containing sialic acids [12]. It has been known that the specific interaction between HA and sialic acid species is one of the determinants of the host range of influenza viruses [13]. Beside its role in the viral attachment, HA is also involved in intracellular fusion between viral envelope and host cell endosome membrane in the endocytotic pathway, by which the virus content is released inside the host cell [14]. The functional maturation of HA is mediated by the cleavage of HA into two disulfide-linked glycopolypeptides, HA1 and HA2 [15], accomplished by trypsin or trypsin-like proteases derived from host cells [16–19]. The membrane fusion is induced by a conformational change in the mature HA, which is triggered at low pH in the endosome, allowing viral ribonucleoprotein complexes to release into the cytoplasm [20,21]. Thus, HA plays a critical role in initiation and progression of influenza virus infection. Influenza virus NA possesses the enzymatic activity that cleaves α-ketosidic linkages between terminal sialic acids and adjacent sugar residues of cellular glycoconjugates [22]. The sialidase activity of NA removes terminal sialic acid residues from HA and NA proteins as well as host cell surface glycoproteins. Since the terminal sialic acid of sialyloligosaccharides is critical for HA binding, the receptor-destroying activity of NA serves to counter the receptor-binding activity of HA. It is quite likely that this activity contributes to prevention of successive superinfection of an infected cell [23]. In the absence of the functional sialidase activity, progeny virions aggregate on the cell surface due to the HA receptor-binding activity and can not be released [24,25]. Thus, NA cleaves sialic acids from the cell surface and facilitates virus release from infected cells. However, it is not clear whether every progeny virion is released as *cell-free* virion to infect the uninfected cells after diffusion into the extracellular environment. Influenza viruses are generally transmitted as *cell-free* viruses from infected to uninfected cell but they may also infect through the cell-to-cell transmission, in particular during local lesion formation.

Here, we examined whether influenza virus transmits from an infected cell to adjacent uninfected cells without virus release. Live cell imaging techniques showed that a recombinant influenza virus, in which the *NA* gene was replaced with the *green fluorescence protein* gene, spreads from an infected cell to adjacent cells forming infected cell clusters. Furthermore, progeny virions remain associated on the surface of infected cell even after budding, and then progeny virions could be passed to adjacent uninfected cells.

Results

Influenza virus can spread in an NA-independent manner to adjacent cells

To examine the transmission pathway of influenza virus, we performed immunofluorescence analyses by using anti-nucleoprotein (NP) polyclonal antibody. Influenza virus can form an infection center even in the presence of oseltamivir, a potent NA inhibitor (commercially known as Tamiflu) [26–28]. Oseltamivir at the concentration of 50 μg/ml completely prevented the release of progeny influenza viruses (Figure 1A). Noted that a large

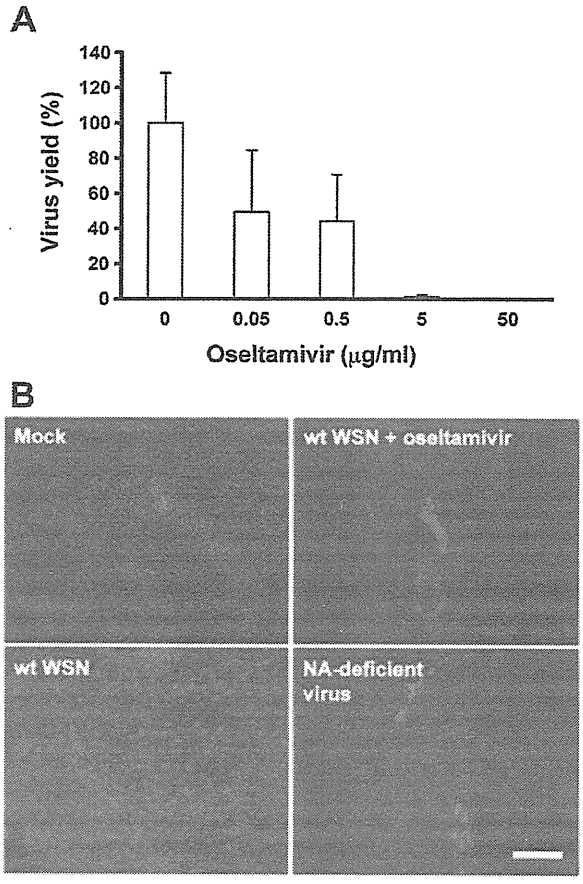

Figure 1. Influenza viruses can spread independent of the NA activity. (A) MDCK cells were infected with influenza virus A/WSN/33 at a multiplicity of infection (MOI) of 0.001 PFU per cell. At 48 hours post infection (hpi), culture supernatant was collected, and then its virus titer was determined by plaque assays. Each result was represented by a value relative to that in the absence of the drug. Error bars indicate standard deviation (s.d.) from 3 independent experiments. (B) Confluent MDCK cells were infected by wild-type influenza virus A/WSN/33 or NA-deficient influenza virus at MOI of 0.0001 in the presence or absence of 50 μg/ml oseltamivir phosphate. NA-deficient influenza virus was generated by reverse genetics as previously described [29]. After incubation at 37°C for 36 hours, immunofluorescence analyses were performed using anti-nucleoprotein (NP) polyclonal antibody and anti-rabbit IgG antibody conjugated to Alexa Fluor 568 (Invitrogen). Scale bar, 100 μm.
doi:10.1371/journal.pone.0028178.g001

number of single fluorescent foci caused by initial infection markedly expanded and formed cell clusters consisting of 5–10 infected cells in an MDCK cell monolayer (Figures 1B and S1), suggesting influenza virus can spread to some extent in the presence of oseltamivir. To verify that NA is not involved in this spreading, we generated an NA-deficient influenza virus by a reverse genetics method as described previously [29,30]. The NA-deficient influenza virus contains a mutated NA segment, in which the NA coding region including a sialidase catalytic domain was replaced with the *enhanced green fluorescent protein (EGFP)* gene [29]. By this replacement, the NA activity is eliminated from the recombinant influenza virus, and *EGFP* can be utilized as a marker for viral infections. Immunofluorescence analyses demonstrated that the NA-deficient influenza virus also forms infected cell

clusters similarly to those formed by wild-type influenza virus in the presence of oseltamivir (Figure 1B). The fluorescence pattern of NP overlapped with the localization of GFP derived from the *EGFP* gene of the NA-deficient influenza virus (Figure S2). Thus, NA-deficient influenza virus can be used to investigate the NA-independent infection pathway of influenza virus.

Next, we performed live cell imaging analyses to directly observe the infection time course of the NA-deficient influenza virus. The GFP fluorescence derived from the NA-deficient influenza virus first appeared in a single cell on an MDCK cell monolayer at 24 hours post infection. The virus started to spread from an infected cell to adjacent cells in 5–6 hours after the first appearance of a GFP-positive cell (Figure 2 and Video S1). The spreading rate was clearly faster than the rate of cell divisions. The mean doubling time of uninfected MDCK cells was 20–24 hours under the condition employed here, and it is expected that the proliferation speed would be much slowly because infected MDCK cells were maintained in the serum-free medium and formed cell monolayer at the high cell density. These suggest that NA-deficient influenza viruses may infect adjacent cells through the cell-to-cell transmission mechanism without apparent production of *cell-free* virions.

Cell-to-cell transmission pathway of influenza viruses is less sensitive to neutralizing antibody

The cell-to-cell virus transmission pathway could be interpreted as one of viral evolving strategies to avoid neutralizing antibody responses [2,31,32]. Therefore, we examined the effect of neutralizing antibody on NA-deficient influenza virus. A polyclonal antibody with the neutralizing activity against influenza virus particles inhibited infection of *cell-free* viruses to less than 50% at the concentration of 0.03%, although the cell cluster formation was observed at the concentration less than 0.01%. On the other hand, the NA-independent transmission of the NA-deficient influenza virus was blocked only when neutralizing antibody was present at the concentration of 0.3% (Figure 3). These results indicated that the NA-independent transmission of influenza viruses is less sensitive to the neutralizing antibody.

NA-independent transmission of influenza virus is HA-dependent

Next, to investigate the mechanism of NA-independent transmission of influenza virus, we examined whether HA is involved in this transmission. In the absence of the NA activity, virus spreading from an infected cell to adjacent cells was dramatically suppressed by omission of trypsin, essential for maturation of HA, from the experimental condition (Figure 4A). The GFP fluorescence derived from NA-deficient influenza virus appeared in a single cell at 24 hours post infection. However, this virus did not spread, but rather disappeared during subsequent 24 hours (Video S2). These observations indicate that the NA-independent cell-to-cell transmission of influenza virus is dependent on HA maturation mediated by trypsin, as is the case for the general *cell-free* transmission of this virus.

To clarify whether virus particles or viral RNP complexes are transmitted to adjacent cells, we examined the effect of amantadine on the cell-to-cell transmission of influenza virus. Amantadine inhibits the early step of uncoating of influenza virus RNP from virion in endosomes [33,34]. For this study, other influenza virus strain, influenza virus A/Udorn/72, was used instead of influenza virus A/WSN/33 because influenza virus A/WSN/33 is highly resistant to amantadine [35]. We confirmed that influenza virus A/Udorn/72 is sensitive to oseltamivir (Figure S3) and could also spread via cell-to-cell transmission independent of the NA activity as did for influenza virus A/WSN/33 (Figures 1B and 4B). In the case of a single administration of amantadine, fluorescent foci derived from infected cells scattered, and the number of single foci was greatly decreased compared

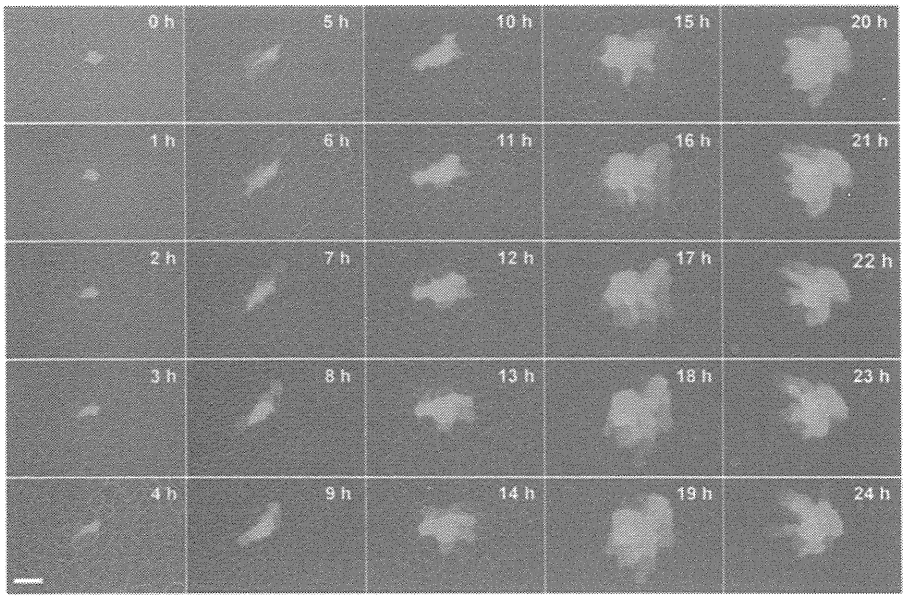

Figure 2. NA-deficient influenza virus spreads through cell-to-cell transmission. Confluent MDCK cells were infected with the NA-deficient influenza virus at MOI of 0.0001. After incubation at 37°C for 24 hours, a single GFP-positive cell, in which the recombinant virus replicated, was found at 1 hour after starting monitoring, and then this cell and its neighborhood were traced during the period from 24 hpi to 48 hpi at interval of 1 hour. Scale bar, 50 μm.
doi:10.1371/journal.pone.0028178.g002

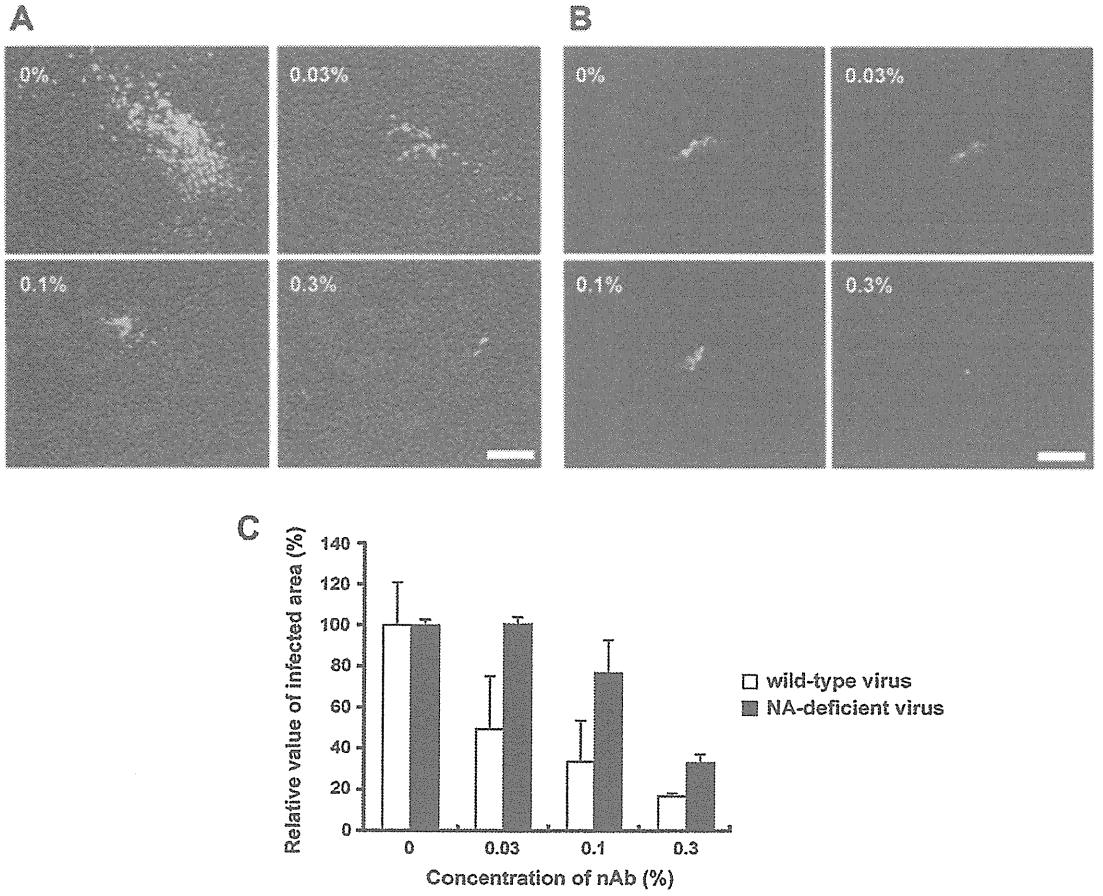

Figure 3. The cell-to-cell transmission of the NA-deficient influenza virus is less sensitive to the neutralizing antibody. (A) Infection of the wild-type and (B) NA-deficient influenza virus were performed in the presence or absence of antiserum containing neutralizing antibodies. Immunofluorescence analyses were performed with cells infected with wild-type influenza virus at 18 hpi using anti-NP antibody and anti-rabbit IgG antibody conjugated to Alexa Fluor 488 (Invitrogen). GFP fluorescence derived from the recombinant virus was observed at 36 hpi. Scale bar, 100 μm. (C) The level of viral spreading was indicated in the graph by measuring NP and GFP derived from wild-type and NA-deficient virus, respectively. Five different microscope fields were taken randomly, and then the intensity of green color was analyzed with ImageJ NIH image processing software. Each result was represented by a value relative to that in the absence of neutralizing antibodies. Error bars indicate s.d. from 3 independent experiments.
doi:10.1371/journal.pone.0028178.g003

with that in the absence of the drugs. In contrast, a single administration of oseltamivir, fluorescent foci formed some clusters and expanded in a time-dependent manner (Figure 4B). This dissimilarity of inhibitory manner was caused by the difference of the sites of action between amantadine and oseltamivir. Amantadine inhibits the replication of influenza A virus by preventing the translocation of vRNP complexes from endosomes to the cytoplasm, whereas oseltamivir has no effects on viral replication itself but inhibits the release of *cell-free* virions from infected host cells. We investigated the inhibitory effect of amantadine on the cell-to-cell transmission of influenza viruses. The formation of infected cell clusters was observed with co-administration of amantadine and oseltamivir, as well as with a single administration of oseltamivir (Figure 4B). However, the quantitative analysis revealed that the size of infected cell clusters with the co-administration were decreased as compared to that with oseltamivir alone (Figure 4C). These observations indicated that the NA activity-independent cell-to-cell transmission of influenza virus was susceptible to the inhibitory effect of amantadine, suggesting that the cell-to-cell transmission undergoes through endocytosis but vRNP complex itself is not incorporated in the infected cells by adjacent cells.

Cell-to-cell transmission occurs on the apical cell membrane

The virus transmission undergoes from infected to uninfected cells through either basolateral [36–38] or apical [39–42] sides. In the case of influenza virus, *cell-free* progeny virions are released only from the apical surface of polarized epithelial cells [43]. This releasing polarity is achieved by directed transport of viral membrane proteins to the apical plasma membrane [44]. Indeed, that HA and NA glycoproteins are associated with lipid rafts, and the raft association has been implicated in apical transport [45,46].

To determine whether or not the cell-to-cell transmission of the NA-deficient influenza virus occurs on the apical surface, we performed transwell assays in the presence of the neutralizing antibody to influenza A viruses. The neutralizing antibody was added to infected MDCK cell monolayer from apical or

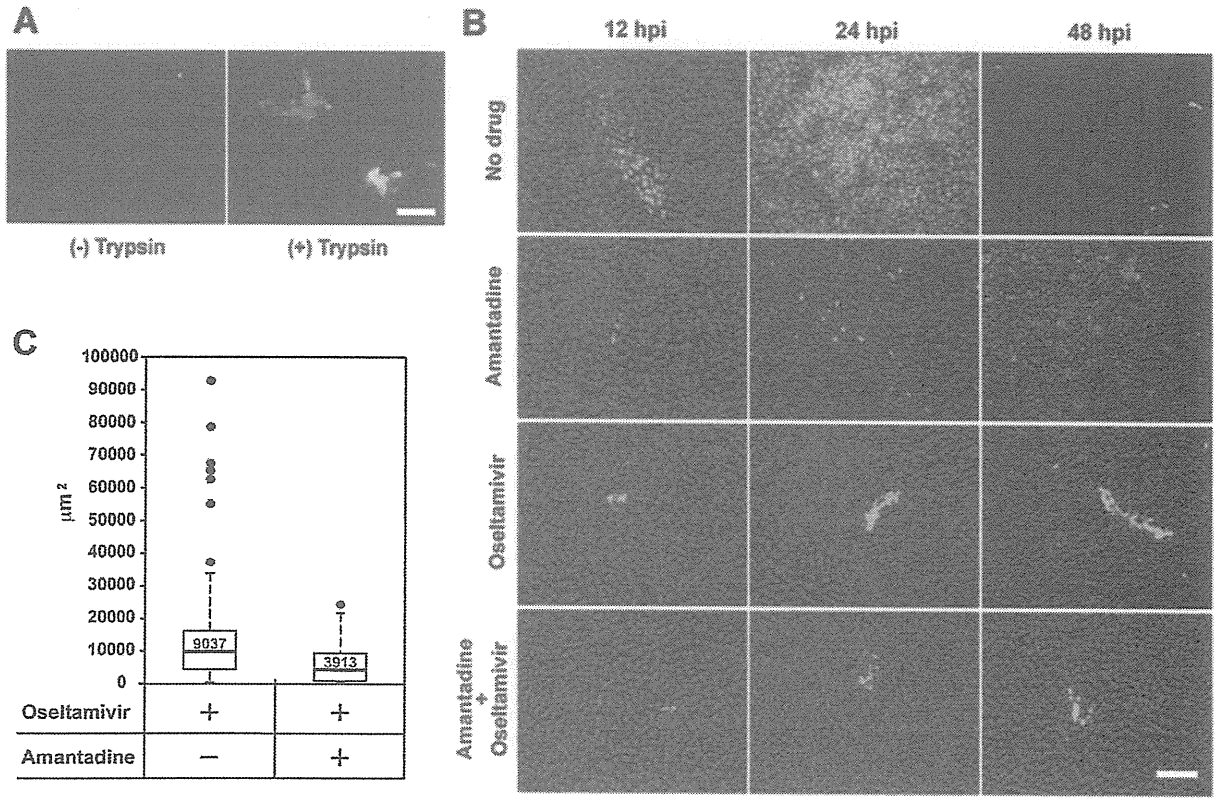

Figure 4. The cell-to-cell transmission of the NA-deficient influenza virus requires functional HA. (A) Confluent MDCK cells were infected with the NA-deficient influenza virus at MOI of 0.0001 in the presence or absence of 1 μg/ml trypsin. GFP fluorescence derived from the recombinant virus was observed at 36 hpi. Scale bar, 100 μm. (B) MDCK cells were infected with influenza virus A/Udorn/72 at moi of 0.0001 in the presence or absence of 50 μM amantadine or 50 μg/ml oseltamivir phosphate. Amantadine at the concentration of 50 μM almost completely inhibited the production of progeny virions (data not shown). After incubation for 12, 24, and 48 h, immunofluorescence analyses were performed using anti-NP antibody and anti-rabbit IgG antibody conjugated to Alexa Fluor 488 (Invitrogen). Viral NP and nuclear DAPI staining are shown in green and blue, respectively. Scale bar, 100 μm. (C) Median sizes of clusters were shown as box plots summarizing sizes of 60 individual infectious foci formed in the presence of oseltamivir alone, or both oseltamivir and amantadine. Immunofluorescence analyses were performed as described in (B) at 24 hpi. Boxes enclose the lower and upper quartiles; thick horizontal lines represent the median; dashed lines indicate the extreme values; and black dots are outliers of individual infectious foci. The size of infectious foci was measured with AxioVision Release 4.7.2 imaging software (Carl Zeiss). Median sizes shown in red letters were clearly different from each other ($p<0.01$).
doi:10.1371/journal.pone.0028178.g004

basolateral side, and the inhibitory effect on the spread of GFP fluorescence derived from the recombinant virus was examined. Addition of high concentrations of the neutralizing antibody from the apical side blocked the cell-to-cell transmission of the NA-deficient influenza virus, whereas the addition from the basolateral side had no effect (Figure 5). These observations indicated that the polarity in the influenza virus budding in the cell-to-cell transmission pathway is apical.

Influenza viruses can not re-infect previously infected cells

Previous report showed that influenza viruses were refractory to superinfection with a second cell-free virus [23]. In the case of the cell-to-cell transmission of influenza virus in the presence of oseltamivir, it is possible that a progeny virion is temporarily bridged by HA between an infected cell and adjacent uninfected cells, since viruses can not be released from infected cell surface due to the inhibition of the NA activity by oseltamivir. The cell-associated progeny virion may have an opportunity to re-infect the previously infected cell, compared to a cell-free progeny virion in the general spreading. Thus, we examined whether influenza viruses can infect the cell which had already been infected, using *ts*53 mutant and wild-type influenza virus A/WSN/33. *ts*53 virus has a substitution mutation from U to C at the nucleotide position of 701 in the PA gene. This substitution introduces an amino acid change from wild-type Leu 226 to Pro 226 and gives a defect in the viral genome replication process [47,48]. At first, cells were infected with *ts*53 virus at moi of 10, and after incubation for 0, 2, 4, 6, and 8 hours, cells were superinfected with wild-type virus at moi of 10. The amount of segment 3 viral RNA (vRNA) encoding PA was determined quantitatively by RT-PCR. Then, using a mutated primer for PCR, we could introduce a *Stu* I site only in the PCR products derived from the wild-type sequence (Figure 6A). Thus, DNA fragments amplified from the wild-type and *ts*53 could be distinguished by *Stu* I digestion. The digested DNA fragments containing 220 and 199 base pairs derived from *ts*53 and wild-type, respectively, were separated through PAGE. After 6 hours or later post infection, re-infection with the second challenging virus hardly occurs in the absence of oseltamivir. However, in the presence of oseltamivir, appearance of wild-type fragment suggests that the re-infection had occurred (Figure 6B). The result indicates

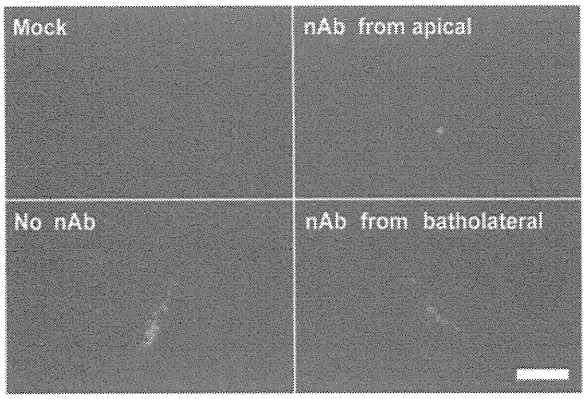

Figure 5. The cell-to-cell transmission of the NA-deficient influenza virus occurs the apical cell surface. Confluent MDCK cells were prepared in transwell inserts and infected with the NA-deficient influenza virus at MOI of 0.0001 in the presence or absence of 0.3% (v/v) antiserum containing neutralizing antibodies (nAb) to influenza A virus. After virus adsorption, the antiserum was added from apical or basolateral side. GFP fluorescence derived from the recombinant virus was observed at 36 hpi. The antiserum added from the apical side could markedly block the cell-to-cell transmission of the NA-deficient influenza virus, whereas the antiserum added from the basolateral side could not. Scale bar, 100 μm.
doi:10.1371/journal.pone.0028178.g005

that progeny virus particles remain on the surface of infected cell even after budding, and can infect the cell previously infected, as well as uninfected cells adjacent to the infected cell, when oseltamivir is present.

Discussion

With the except for the virus which spreads through the cell-cell fusion transmission, virus infection is initiated by the binding of *cell-free* virions to their host cells. Recently, the virus transmission mechanism from an infected cell to adjacent cells without virus diffusion into the extracellular environment is highlighted from the aspect of its significance in virus spreading in the presence of antibodies [1,2]. This antibody-insensitive pathway is often called cell-to-cell transmission [2]. The cell-to-cell transmission may be categorized into two pathways, *i.e.*, transmission of *cell-free* virions to adjacent uninfected cells, and transmission of progeny virions associated on the surface of an infected cell even after budding through narrow synaptic space between an infected cell and adjacent uninfected cells. As an example of the former mechanism, *cell-free* vaccinia virus particles associated with the filopodium of an infected cell are repelled toward neighboring uninfected cells by inducing the formation of actin filament [3]. Several cases have been reported for the latter mechanism: Immunotropic viruses including retroviruses utilize the immunological synapses [4–7]. Immune cells are not constitutively polarized, but contain the machinery that directs their secretory apparatus towards a cell that is involved in an immunological synapse. This machinery can be subverted by retroviruses containing human immunodeficiency virus (HIV). An HIV-infected cell can polarize viral budding towards a target cell expressing receptor through a structure called a virological synapse. Virions bud from an infected cell into a synaptic cleft, from which they fuse with the target-cell plasma membrane [49–52]. The progeny virions of HCV are trapped between infected and uninfected cell membranes at the tight junction. Using Claudin-1 known as a component of the tight junction and one of the entry factors of HCV [8], virions fuse with and penetrate uninfected target cells [31]. Therefore, HCV may acquire the ability to spread within polarized liver epithelium. Thus, the cell-to-cell transmission certainly plays significant roles for the dissemination of several enveloped viruses. However, the cell-to-cell transmission of influenza virus has not been discussed well. Here, we have shown that influenza virus spreads by forming infected cell clusters even in the presence of an NA inhibitor. Live cell imaging clearly showed that influenza virus lacking the NA activity spreads from an infected cell to adjacent cells through the cell-to-cell transmission mechanism (Figure 2). This was also the case for wild-type influenza virus during early phases of infection (Figure 4B). In the cell-to-cell transmission of influenza virus, progeny virions could remain associated with the surface of infected cell even after budding, and then these progeny virions can be passed on to adjacent uninfected cells.

We showed that the cell-to-cell transmission of the NA-deficient influenza virus depends on functional HA. The viral spreading was dramatically suppressed without HA activation by trypsin treatment (Figure 4A). Moreover, the cell-to-cell transmission was also blocked by amantadine, which inhibits the acidification of endosomes required for uncoating of influenza virus particles in endosomes [33,34]. These findings indicate that functional HA and endosome acidification by M2 ion channel are required for the cell-to-cell influenza virus transmission, thereby allowing viruses to enter the adjacent cells through the endocytotic pathway (Figure 4).

Our findings showed that the NA-deficient influenza virus is not diffused into the extracellular environment. The viral spreading in the absence of oseltamivir appears to be much faster compared to the viral spreading in the presence of the drug, suggesting that NA could be involved in determination of spreading speed (Figure 4B). The NA activity prevented progeny virions from entering cells which virus came from (Figure 6), implying that progeny virus particles should be transmitted to adjacent uninfected cells. The cell-to-cell transmission started in early phase of infection, and the virus spread through diffusion of *cell-free* viruses (Figure 4B). Indeed, it was reported that the cell-to-cell transmission is a rapid spreading pathway in the case of vaccinia virus [3]. Vaccinia virus induces a blocking mechanism of superinfection and thereby infects to adjacent uninfected cells efficiently. In early phases of vaccinia virus infection, viral proteins A33 and A36 are expressed at the infected cell surface. Once *cell-free* virus particles contact the filopodium, the A33/A36 complex induces the formation of actin filament, which causes this superinfected virion to be repelled toward uninfected cells [3]. Influenza viruses can re-infect the cells previously infected in the presence of oseltamivir (Figure 6), suggesting that a progeny virion may be bridged by HA between infected and adjacent uninfected cells temporarily. Thus, in the case of the cell-to-cell transmission of influenza virus, we propose that progeny virions associated with the surface of infected cells even after budding are directed to adjacent uninfected cells. The cell-to-cell transmission mechanism of influenza virus is distinctly different from that of vaccinia virus in the infecting virus status: Infected cell-associated virions and *cell-free* virions are involved in the cell-to-cell transmission of influenza virus and vaccinia virus, respectively. The strategy for influenza virus appears to be similar to that for HCV. HCV progeny virions budded from an infected cell are trapped between infected and uninfected adjacent cell membranes at the tight junction. HCV virions then, enter into adjacent cells through endocytosis and low pH-dependent membrane fusion using Claudin-1 [8]. The cell-to-cell transmission of influenza virus also required functional HA and endosome acidification by M2 ion channel. However, it has not been reported that HCV has a gene encoding a receptor destroying

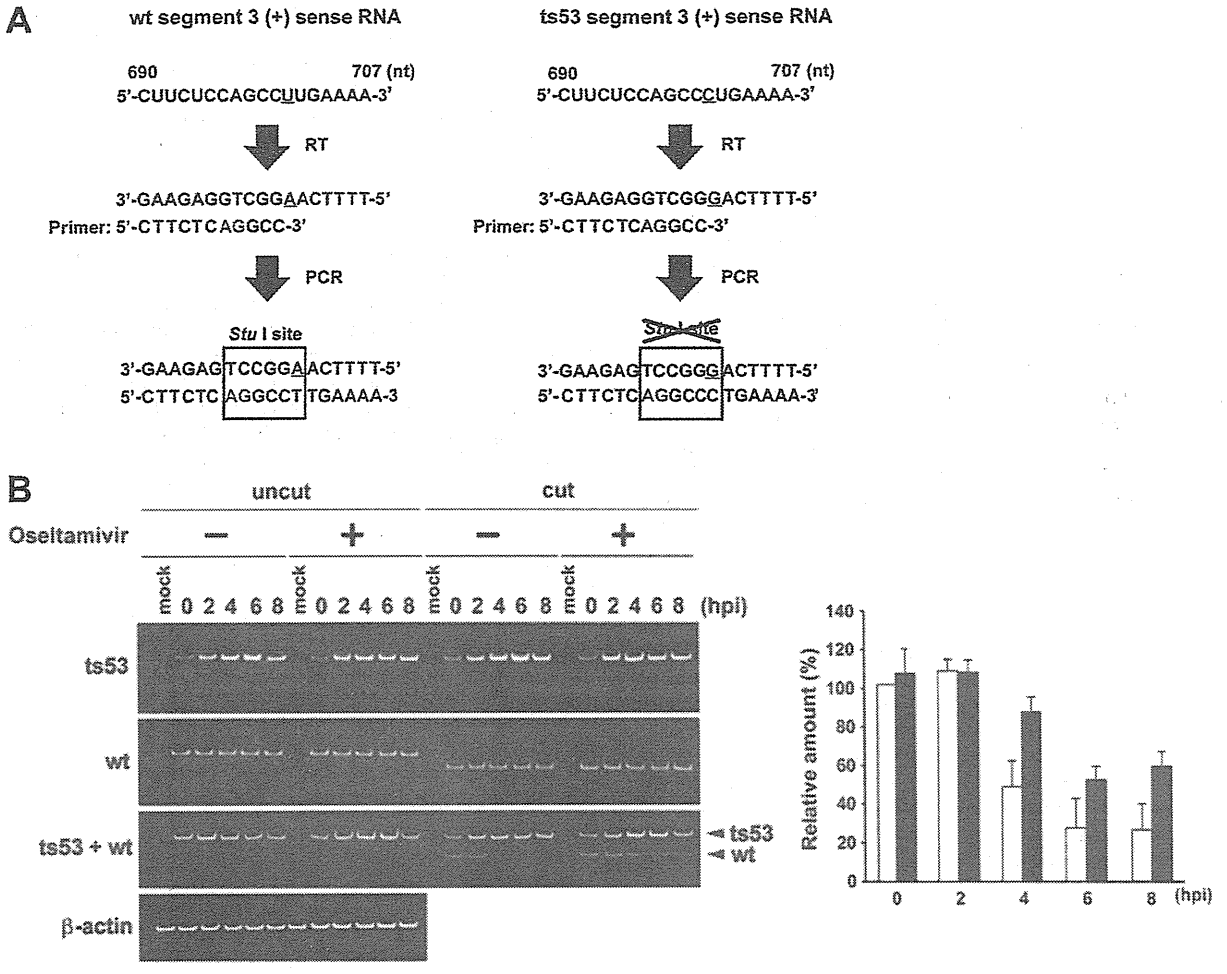

Figure 6. Influenza viruses can not re-infect previously infected cells. (A) A method for determination of the amount of segment 3 genome derived from *ts*53 and wild-type. Total RNA was reverse-transcribed with the primer PA-895-rev, which is complementary to the segment 3 positive-sense RNA. The cDNA was amplified by PCR using primers, PA-895-rev and PA-695-cut partially corresponding to segment 3 positive sense RNA between the nucleotide sequence positions 678 to 700 except for 696 and 697, which are shown in red letters. Since segment 3 of *ts*53 has a substitution mutation from U to C at the nucleotide position of 701, the PCR product derived from wild-type could be digested by *Stu* I but not that from *ts*53. Then, PCR products were digested with *Stu* I and separated through 8% PAGE. (B) Detection of the genome of the segment 3 derived from *ts*53 or wild-type. At 3 hours post superinfection of wild-type virus, total RNA was extracted, and semi-quantitative RT-PCR was performed. Subsequently, the amplified DNA products were digested with *Stu* I and separated through 8% PAGE. Large and small fragments derived from *ts*53 and wild-type viruses were 220 and 199 base pairs, respectively. The relative amount of wild-type segment 3 to that at 0 hour in the absence of oseltamivir phosphate was shown in the graph. Error bars indicate S.D. from 3 independent experiments. White bar, in the absence of oseltamivir phosphate; black bar, in the presence of oseltamivir phosphate.
doi:10.1371/journal.pone.0028178.g006

enzyme similar to NA of influenza virus. We speculated that HCV progeny particles are bridged between infected and adjacent uninfected cells temporarily like influenza virus in the presence of oseltamivir. Progeny influenza virus particles could be transmitted to adjacent uninfected cells efficiently in the presence of the NA activity, suggesting that the cell-to-cell transmission of influenza virus is more strategic than that of HCV.

Our findings raise an interesting question as to what is the biological significance of cell-to-cell transmission for influenza virus infection *in vivo*. Until now, it had been believed that influenza virus was released from infected cells as *cell-free* virions and then spread from cell to cell as well as from organism to organism. The transmission mode by *cell-free* virions undergoes the extremely high-speed of its diffusion and causes epidemic or pandemic infection. The tropism in an infected animal body is generally restricted to respiratory tract or lung and its periphery, and the requirement of a trypsin-like protease has been generally described for the reason of the restriction. It is possible that the cell-to-cell transmission mode may play a significant role for the virus spreading inside of organism, although *cell-free* influenza virions are causative of high-speed spreading. At the least, the limited but distinct level of infection followed by replication could provide some opportunity to generate influenza virus variants. It is an open question whether the cell-to-cell transmission mode is involved in the pathogenesis caused by influenza virus infection *in vivo*.

The existence of cell-to-cell transmission pathway gives a caution when NA inhibitors are used, because NA inhibitors may not be sufficient to completely block the spread of influenza

virus in local microenvironments. Since this cell-to-cell transmission pathway exists, development of antiviral therapeutic strategies in addition to NA inhibitors is highly recommended.

Materials and Methods

Cells and viruses

Madin-Darby canine kidney (MDCK) cells were kindly gifted by A. Ishihama (Hosei University), and maintained in minimal essential medium (MEM) (Nissui) containing 10% fetal bovine serum. Human embryonic kidney 293T cells were kindly gifted by Y. Kawaoka (University of Tokyo), and maintained in Dulbecco modified Eagle medium (DMEM) (Nissui) supplemented with 10% fetal bovine serum. Influenza virus A/Udorn/72 was grown in allantoic sacs of 11 day-old embryonated eggs (MIYAKE HATCHERY). Wild-type influenza virus A/WSN/33 and *ts*53 mutant were used after single-plaque isolation. MDCK cells were infected with influenza virus A/WSN/33 or *ts*53 at a multiplicity of infection (MOI) of 0.1 PFU/cell, and incubated at 37°C and 34°C, respectively. After incubation for 24 h, the culture fluid was harvested and centrifuged at 1,700× *g* for 10 min. The virus suspension was stored at −80°C until use.

Antibodies

The production of rabbit polyclonal anti-NP antibody was described previously [53], and this antibody was used as a primary antibody for indirect immunofluorescence assay. A goat anti-rabbit IgG antibody conjugated to Alexa Fluor 488 or Alexa Fluor 568 was purchased from Invitrogen and used as a secondary antibody for indirect immunofluorescence assay. A polyclonal antibody against influenza A virus was obtained from 2-month-old female rabbit immunized with 250 μg of purified virions of influenza virus strain A/Puerto Rico/8/34 [54]. The generation of antibodies was boosted three times and used as neutralizing antibodies to block the influenza virus infection.

Determination of the inhibition effect of oseltamivir on virus production

MDCK cells were infected with influenza virus A/WSN/33 at a multiplicity of infection (MOI) of 0.001 PFU per cell. After virus adsorption at 37°C for 1 hour, the cells were washed with serum-free MEM and incubated at 37°C with maintenance medium (MEM containing vitamins and 0.1% BSA) containing oseltamivir. At 48 hours post infection (hpi), culture supernatant was collected, and then its viral titer was determined by plaque assays.

Generation of neuraminidase (NA)-deficient viruses

An NA-deficient influenza virus possessing the terminal sequences of NA segment but lacking the NA coding region, which was replaced with *enhanced green fluorescent protein (EGFP)* gene, was generated by reverse genetics as described previously [29,30]. For reverse genetics, we used plasmids containing cDNAs of the influenza virus A/WSN/33 viral genome under the control of the human RNA polymerase I promoter (referred to as Pol I plasmids). Briefly, 293T cells were transfected with seven Pol I plasmids for production of all vRNA segments of influenza virus A/WSN/33 and one for the mutant NA vRNA segment containing *EGFP* ORF, together with protein expression vectors for PB2, PB1, PA, and NP controlled by the chicken β-actin promoter (pCAGGS). TransIT-293 (Mirus) was used for transfection. At 24 hours post transfection, recombinant viruses were harvested from the cell surface using bacterial NA derived from *Clostridium perfringens* (sigma). MDCK cells were infected with harvested recombinant viruses treated with *N*-tosyl-L-phenylalanine chloromethyl ketone (TPCK)-trypsin (1 μg/ml). After confirmation of GFP fluorescence derived from amplified recombinant virus genomes at 48 hours after infection, the recombinant viruses on the cell surface were collected using bacterial NA. The viral titer of recombinant viruses was determined by counting the number of infected foci using a fluorescence microscopy (Carl Zeiss).

Indirect immunofluorescence assay

Cells on coverslips were fixed with 4% paraformaldehyde in phosphate-buffered saline (PBS) for 10 min and permeabilized with 0.2% NP-40 in PBS. The coverslips were soaked in 1% bovine serum albumin in PBS, and then incubated at room temperature for 1 hour with a primary antibody. After being washed twice with PBS, the coverslips were incubated at room temperature for 1 hour with a secondary antibody. The coverslips were then incubated at room temperature for 5 min with 3 μM 4′,6′-diamidino-2-phenylindole (DAPI) and finally mounted on glass plates, and cells were observed under the fluorescence microscope.

Live cell imaging analyses

Living cells were analyzed using BioStation ID system (GE Healthcare). Confluent MDCK cells were infected with the NA-deficient influenza virus at the multiplicity of infection (MOI) of 0.0001 in the presence or absence of 1 μg/ml TPCK-trypsin. At 24 hours post infection, culture dishes containing infected cells were set into the chamber of BioStaion ID system, which was maintained at 37°C under 5% CO_2 and 95% humidity. Then, images were acquired during next 24 hours at interval with 1 hour. The excitation wavelength was controlled by a manual filter wheel equipped with filters suitable for enhanced green fluorescence protein (EGFP).

Transwell assay

Confluent MDCK cell monolayer was prepared on transwell inserts (BD Falcon, pore size 0.4 μm) and infected with the NA-deficient influenza virus at MOI of 0.0001. After virus adsorption at 37°C for 1 hour, the cell monolayer was washed with serum-free MEM, and maintenance medium was added into both sides within the transwells. The neutralizing antibody to influenza A virus was added into the inside or the outside of transwell inserts with the maintenance medium. Subsequently, cells were incubated at 37°C for 36 hours followed by analyses using the fluorescence microscopy.

RT-PCR

*ts*53 virus has a substitution mutation from U to C at the nucleotide position of 701 in the *PA* gene. This substitution introduces an amino acid change from wild-type Leu 226 to Pro 226 and gives a defect in the viral genome replication process [48]. However, under the permissive temperature, the level of viral genome replication is no difference between wild-type and *ts*53 [47]. To discriminate the genome of wild-type and that of *ts*53, total RNA was reverse-transcribed by reverse transcriptase (TOYOBO) with PA-895-rev (5′-TTAATTTTAAGGCATC-CATCAGCAGG-3′), which is complementary to the segment 3 positive sense RNA. The cDNA was amplified by PCR using primers, PA-895-rev and PA-695-cut (5′-TCTCCCGCCA-AACTTCTCAGGCC-3′) partially corresponding to segment 3 positive sense RNA between nucleotide sequence positions 678 to 700 except for nucleotide positions 696 and 697. Since segment 3 of *ts*53 has a substitution mutation from U to C at the nucleotide position of 701, the PCR product derived from wild-type was digested by *Stu* I but not that from *ts*53. After PCR reactions, PCR

products were digested with *Stu* I and separated through PAGE. Large and small fragments derived from *ts*53 and wild-type viruses were 220 and 199 base pairs, respectively. DNA was stained with GelRed (BIOTIUM) and visualized by UV illumination.

Supporting Information

Figure S1 Formation of cell cluster caused by initial infection. MDCK cells were infected with influenza virus A/WSN/33 at moi of 0.0003 in the presence or absence of 50 μg/ml oseltamivir phosphate. After incubation for 8 and 24 h, immunofluorescence analyses were performed using anti-NP antibody and anti-rabbit IgG antibody conjugated to Alexa Fluor 488 (Invitrogen). Nuclear DAPI and viral NP staining patterns are shown in blue and green, respectively. Enlarged views are shown in red borders. Scale bar, 100 μm.
(TIF)

Figure S2 The expression of GFP derived from NA-deficient influenza virus overlapped with the localization of NP. MDCK cells were infected with NA-deficient influenza viruses at MOI of 0.0001. After incubation at 37°C for 48 hours, immunofluorescence analyses were performed using anti-NP antibody. Scale bar, 100 μm.
(TIF)

Figure S3 Influenza virus A/Udorn/72 was sensitive to oseltamivir. MDCK cells were infected with influenza virus A/Udorn/72 at a MOI of 0.001 PFU per cell. At 36 hpi, the culture supernatant was collected, and then its virus titer was determined by plaque assays. Each result was represented by a value relative to that in the absence of the drug. Error bars indicate s.d. from 3 independent experiments.
(TIF)

Video S1 NA-deficient influenza virus spreads through cell-to-cell transmission. Confluent MDCK cells were infected with NA-deficient influenza virus at MOI of 0.0001 in the presence of trypsin. After incubation at 37°C for 24 hours, a single GFP-positive cell and its vicinity were traced it during the period from 24 hpi to 48 hpi at interval of 1 hour. Live cell imaging data analyses was performed by Biostation ID (GE healthcare). Scale bar, 50 μm.
(MOV)

Video S2 NA-deficient influenza virus does not spread in the absence of trypsin. Confluent MDCK cells were infected with the NA-deficient influenza virus at MOI of 0.0001 in the absence of trypsin. After incubation at 37°C for 24 hours, a single GFP-positive cell was detected, and then this cell and neighborhood cells was traced during the period from 24 hpi to 48 hpi at interval of 1 hour. Live cell imaging data analyses were performed by Biostation ID (GE healthcare). Scale bar, 50 μm.
(MOV)

Acknowledgments

We thank A. Ishihama (Hosei University) for MDCK cells, Y. Kawaoka (University of Tokyo) for 293T cells. We also thank K. Ho for his careful proofreading of the manuscript. We are grateful to A. Kawaguchi (Kitasato University and University of Tsukuba) for his valuable discussion during the course of this work.

Author Contributions

Conceived and designed the experiments: KM TH KN. Performed the experiments: KM TH. Analyzed the data: KM TH KN. Contributed reagents/materials/analysis tools: TH. Wrote the paper: KM TH KN.

References

1. Sattentau Q (2008) Avoiding the void: cell-to-cell spread of human viruses. Nat Rev Microbiol 6: 815–826.
2. Mothes W, Sherer NM, Jin J, Zhong P (2010) Virus Cell-to-Cell Transmission. J Virol 84: 8360–8368.
3. Doceul V, Hollinshead M, van der Linden L, Smith GL (2010) Repulsion of superinfecting virions: a mechanism for rapid virus spread. Science 327: 873–876.
4. Igakura T, Stinchcombe JC, Goon PK, Taylor GP, Weber JN, et al. (2003) Spread of HTLV-I between lymphocytes by virus-induced polarization of the cytoskeleton. Science 299: 1713–1716.
5. Dustin M (2003) Viral spread through protoplasmic kiss. Nat Cell Biol 5: 271–272.
6. Hübner W, McNerney GP, Chen P, Dale BM, Gordon RE, et al. (2009) Quantitative 3D video microscopy of HIV transfer across T cell virological synapses. Science 323: 1743–1747.
7. Pais-Correia AM, Sachse M, Guadagnini S, Robbiati V, Lasserre R, et al. (2010) Biofilm-like extracellular viral assemblies mediate HTLV-1 cell-to-cell transmission at virological synapses. Nat Med 16: 83–89.
8. Evans MJ, von Hahn T, Tscherne DM, Syder AJ, Panis M, et al. (2007) Claudin-1 is a hepatitis C virus co-receptor required for a late step in entry. Nature 446: 801–805.
9. Ploss A, Evans MJ, Gaysinskaya VA, Panis M, You H, et al. (2009) Human occludin is a hepatitis C virus entry factor required for infection of mouse cells. Nature 457: 882–886.
10. Barton ES, Forrest JC, Connolly JL, Chappell JD, Liu Y, et al. (2001) Junction adhesion molecule is a receptor for reovirus. Cell 104: 441–451.
11. Balfe P, McKeating JA (2009) The complexities of hepatitis C virus entry. J Hepatol 51: 609–611.
12. Wiley DC, Skehel JJ (1987) The structure and function of the hemagglutinin membrane glycoprotein of influenza virus. Annu Rev Biochem 56: 365–394.
13. Suzuki Y, Ito T, Suzuki T, Holland RE, Chambers TM, et al. (2000) Sialic acid species as a determinant of the host range of influenza A viruses. J Virol 74: 11825–11831.
14. Skehel JJ, Bayley PM, Brown EB, Martin SR, Waterfield MD, et al. (1982) Changes in the conformation of influenza virus hemagglutinin at the pH optimum of virus-mediatedmozawa T, membrane fusion. P Natl Acad Sci Usa 79: 968–972.
15. Skehel JJ, Waterfield MD (1975) Studies on the primary structure of the influenza virus hemagglutinin. P Natl Acad Sci Usa 72: 93–97.
16. Sato M, Yoshida S, Iida K, Tomozawa T, Kido H, et al. (2003) A novel influenza A virus activating enzyme from porcine lung: purification and characterization. Biol Chem 384: 219–227.
17. Lazarowitz SG, Choppin PW (1975) Enhancement of the infectivity of influenza A and B viruses by proteolytic cleavage of the hemagglutinin polypeptide. Virology 68: 440–454.
18. Klenk HD, Rott R, Orlich M, Blödorn J (1975) Activation of influenza A viruses by trypsin treatment. Virology 68: 426–439.
19. Kido H, Yokogoshi Y, Sakai K, Tashiro M, Kishino Y, et al. (1992) Isolation and characterization of a novel trypsin-like protease found in rat bronchiolar epithelial Clara cells. A possible activator of the viral fusion glycoprotein. J Biol Chem 267: 13573–13579.
20. Bullough PA, Hughson FM, Skehel JJ, Wiley DC (1994) Structure of influenza haemagglutinin at the pH of membrane fusion. Nature 371: 37–43.
21. Tamm LK, Han X, Li Y, Lai AL (2002) Structure and function of membrane fusion peptides. Biopolymers 66: 249–260.
22. Air GM, Laver WG (1989) The neuraminidase of influenza virus. Proteins 6: 341–356.
23. Huang IC, Li W, Sui J, Marasco W, Choe H, et al. (2008) Influenza A virus neuraminidase limits viral superinfection. J Virol 82: 4834–4843.
24. Palese P, Tobita K, Ueda M, Compans RW (1974) Characterization of temperature sensitive influenza virus mutants defective in neuraminidase. Virology 61: 397–410.
25. Shibata S, Yamamoto-Goshima F, Maeno K, Hanaichi T, Fujita Y, et al. (1993) Characterization of a temperature-sensitive influenza B virus mutant defective in neuraminidase. J Virol 67: 3264–3273.
26. Gubareva LV, Nedyalkova MS, Novikov DV, Murti KG, Hoffmann E, et al. (2002) A release-competent influenza A virus mutant lacking the coding capacity for the neuraminidase active site. J Gen Virol 83: 2683–2692.
27. Nedyalkova MS, Hayden FG, Webster RG, Gubareva LV (2002) Accumulation of defective neuraminidase (NA) genes by influenza A viruses in the presence of NA inhibitors as a marker of reduced dependence on NA. J Infect Dis 185: 591–598.
28. Lew W, Chen X, Kim CU (2000) Discovery and development of GS 4104 (oseltamivir): an orally active influenza neuraminidase inhibitor. Curr Med Chem 7: 663–672.

29. Fujii Y, Goto H, Watanabe T, Yoshida T, Kawaoka Y (2003) Selective incorporation of influenza virus RNA segments into virions. P Natl Acad Sci Usa 100: 2002–2007.
30. Shinya K, Fujii Y, Ito H, Ito T, Kawaoka Y (2004) Characterization of a neuraminidase-deficient influenza a virus as a potential gene delivery vector and a live vaccine. J Virol 78: 3083–3088.
31. Timpe JM, Stamataki Z, Jennings A, Hu K, Farquhar MJ, et al. (2008) Hepatitis C virus cell-cell transmission in hepatoma cells in the presence of neutralizing antibodies. Hepatology 47: 17–24.
32. Gupta P, Balachandran R, Ho M, Enrico A, Rinaldo C (1989) Cell-to-cell transmission of human immunodeficiency virus type 1 in the presence of azidothymidine and neutralizing antibody. J Virol 63: 2361–2365.
33. Pinto LH, Holsinger LJ, Lamb RA (1992) Influenza virus M2 protein has ion channel activity. Cell 69: 517–528.
34. Davies WL, Grunert RR, Haff RF, McGahen JW, Neumayer EM, et al. (1964) Antiviral Activity of 1-Adamantanamine (Amantadine). Science 144: 862–863.
35. Takeda M, Pekosz A, Shuck K, Pinto LH, Lamb RA (2002) Influenza a virus M2 ion channel activity is essential for efficient replication in tissue culture. J Virol 76: 1391–1399.
36. Chodosh J, Gan Y, Holder VP, Sixbey JW (2000) Patterned entry and egress by Epstein-Barr virus in polarized CR2-positive epithelial cells. Virology 266: 387–396.
37. Fuller S, von Bonsdorff CH, Simons K (1984) Vesicular stomatitis virus infects and matures only through the basolateral surface of the polarized epithelial cell line, MDCK. Cell 38: 65–77.
38. Schlie K, Maisa A, Freiberg F, Groseth A, Strecker T, et al. (2010) Viral protein determinants of Lassa virus entry and release from polarized epithelial cells. J Virol 84: 3178–3188.
39. Blau DM, Compans RW (1995) Entry and release of measles virus are polarized in epithelial cells. Virology 210: 91–99.
40. Brock SC, Goldenring JR, Crowe JE, Jr. (2003) Apical recycling systems regulate directional budding of respiratory syncytial virus from polarized epithelial cells. Proc Natl Acad Sci U S A 100: 15143–15148.
41. Roberts SR, Compans RW, Wertz GW (1995) Respiratory syncytial virus matures at the apical surfaces of polarized epithelial cells. J Virol 69: 2667–2673.
42. Tseng CT, Tseng J, Perrone L, Worthy M, Popov V, et al. (2005) Apical entry and release of severe acute respiratory syndrome-associated coronavirus in polarized Calu-3 lung epithelial cells. J Virol 79: 9470–9479.
43. Nayak DP, Hui EK, Barman S (2004) Assembly and budding of influenza virus. Virus Research 106: 147–165.
44. Carrasco M, Amorim MJ, Digard P (2004) Lipid raft-dependent targeting of the influenza A virus nucleoprotein to the apical plasma membrane. Traffic 5: 979–992.
45. Cresawn KO, Potter BA, Oztan A, Guerriero CJ, Ihrke G, et al. (2007) Differential involvement of endocytic compartments in the biosynthetic traffic of apical proteins. Embo J 26: 3737–3748.
46. Guerriero CJ, Lai Y, Weisz OA (2008) Differential sorting and Golgi export requirements for raft-associated and raft-independent apical proteins along the biosynthetic pathway. J Biol Chem 283: 18040–18047.
47. Kawaguchi A, Naito T, Nagata K (2005) Involvement of influenza virus PA subunit in assembly of functional RNA polymerase complexes. J Virol 79: 732–744.
48. Sugiura A, Ueda M, Tobita K, Enomoto C (1975) Further isolation and characterization of temperature-sensitive mutants of influenza virus. Virology 65: 363–373.
49. Guyader M, Kiyokawa E, Abrami L, Turelli P, Trono D (2002) Role for human immunodeficiency virus type 1 membrane cholesterol in viral internalization. J Virol 76: 10356–10364.
50. Jolly C, Sattentau QJ (2005) Human immunodeficiency virus type 1 virological synapse formation in T cells requires lipid raft integrity. J Virol 79: 12088–12094.
51. Phillips DM (1994) The role of cell-to-cell transmission in HIV infection. AIDS 8: 719–731.
52. Sato H, Orenstein J, Dimitrov D, Martin M (1992) Cell-to-cell spread of HIV-1 occurs within minutes and may not involve the participation of virus particles. Virology 186: 712–724.
53. Kawaguchi A, Momose F, Nagata K (2011) Replication-coupled and host factor-mediated encapsidation of the influenza virus genome by viral nucleoprotein. J Virol 85: 6197–6204.
54. Watanabe K, Handa H, Mizumoto K, Nagata K (1996) Mechanism for inhibition of influenza virus RNA polymerase activity by matrix protein. J Virol 70: 241–247.

Journal of General Virology (2011), **92**, 1416–1427 DOI 10.1099/vir.0.030403-0

Characterization of influenza A viruses isolated from wild waterfowl in Zambia

Edgar Simulundu,[1] Akihiro Ishii,[1,2] Manabu Igarashi,[1] Aaron S. Mweene,[3] Yuka Suzuki,[1,2] Bernard M. Hang'ombe,[4] Boniface Namangala,[4] Ladslav Moonga,[4] Rashid Manzoor,[1] Kimihito Ito,[1] Ichiro Nakamura,[1,3] Hirofumi Sawa,[1,3] Chihiro Sugimoto,[1,3] Hiroshi Kida,[1,5,6] Chuma Simukonda,[7] Wilbroad Chansa,[7] Jack Chulu[7] and Ayato Takada[1,2]

Correspondence
Ayato Takada
atakada@czc.hokudai.ac.jp

[1]Hokkaido University Research Center for Zoonosis Control, Kita-20, Nishi-10, Kita-ku, Sapporo 001-0020, Japan

[2]Hokudai Center for Zoonosis Control in Zambia, School of Veterinary Medicine, The University of Zambia, PO Box 32379, Lusaka, Zambia

[3]Department of Disease Control, School of Veterinary Medicine, The University of Zambia, PO Box 32379, Lusaka, Zambia

[4]Department of Paraclinical Studies, School of Veterinary Medicine, The University of Zambia, PO Box 32379, Lusaka, Zambia

[5]Department of Disease Control, Graduate School of Veterinary Medicine, Hokkaido University, Sapporo 060-0818, Japan

[6]Japan Science and Technology Agency Basic Research Programs, Saitama, Japan

[7]Zambia Wildlife Authority, Kafue Road, Private Bag 1, Chilanga, Zambia

Although the quest to clarify the role of wild birds in the spread of the highly pathogenic H5N1 avian influenza virus (AIV) has yielded considerable data on AIVs in wild birds worldwide, information regarding the ecology and epidemiology of AIVs in African wild birds is still very limited. During AIV surveillance in Zambia (2008–2009), 12 viruses of distinct subtypes (H3N8, H4N6, H6N2, H9N1 and H11N9) were isolated from wild waterfowl. Phylogenetic analyses demonstrated that all the isolates were of the Eurasian lineage. Whilst some genes were closely related to those of AIVs isolated from wild and domestic birds in South Africa, intimating possible AIV exchange between wild birds and poultry in southern Africa, some gene segments were closely related to those of AIVs isolated in Europe and Asia, thus confirming the inter-regional AIV gene flow among these continents. Analysis of the deduced amino acid sequences of internal proteins revealed that several isolates harboured particular residues predominantly observed in human influenza viruses. Interestingly, the isolates with human-associated residues exhibited higher levels of virus replication in the lungs of infected mice and caused more morbidity as measured by weight loss than an isolate lacking such residues. This study stresses the need for continued monitoring of AIVs in wild and domestic birds in southern Africa to gain a better understanding of the emergence of strains with the potential to infect mammals.

Received 9 January 2011
Accepted 28 February 2011

INTRODUCTION

Avian influenza viruses (AIVs) are zoonotic pathogens maintained in nature mainly in wild aquatic birds (Olsen *et al.*, 2006; Webster *et al.*, 1992). Viruses of 16 different haemagglutinin (HA) (H1–H16) and nine neuraminidase (NA) (N1–N9) subtypes have been identified in waterfowl reservoirs. These viruses are usually non-pathogenic for their natural hosts. It is generally accepted that highly pathogenic AIVs (HPAIVs), particularly of the H5 and H7 subtypes, emerge from low-pathogenic AIV (LPAIV) precursors once introduced into poultry and that they may not be harboured by wild birds (Capua & Alexander, 2006; Röhm *et al.*, 1995). After emerging in China in 1996, H5N1 HPAIV spread rapidly throughout Asia, Europe, the

The GenBank/EMBL/DDBJ accession numbers for the sequences reported in this study are AB569476–AB569571.

Supplementary data on the phylogenetic relationships of AIVs from wild birds in Zambia are available with the online version of this paper.

Middle East and Africa, causing unprecedented outbreaks in wild birds, poultry and occasional human infections that have risen to pose a significant pandemic threat (Ducatez *et al.*, 2006; Li *et al.*, 2004; Smith *et al.*, 2006; Wang *et al.*, 2008). The rapid spread of the H5N1 HPAIV and the detection of H5N2 AIVs with an HP viral genotype in healthy wild waterfowl in Africa (Gaidet *et al.*, 2008) have heightened the possibility of the existence of a wild-bird reservoir for HPAIVs and underscore the need to improve our current understanding of the eco-epidemiological dynamics of AIVs in nature.

As early as 1961, Africa recorded the first outbreak of HPAIV in wild birds, which caused the death of approximately 1300 common terns (Capua & Alexander, 2006). Until 2004 when H5N2 HPAIV caused an outbreak in South African ostriches, there had been no reported cases of HP avian influenza in Africa. The continent's first experience with the Asian-origin H5N1 HPAIV was in 2006 in Nigeria (Ducatez *et al.*, 2006). The virus has since spread to several African countries, affecting a range of avian species with sporadic spillover into humans. Egypt is the African country that has recorded the highest number of human infections with the H5N1 HPAIV to date, with 115 confirmed cases, of which 38 were fatal (World Health Organization, 2010). Despite the significance of these events, which pose a serious threat to animal and public health, as well as to food security in Africa, very little is known about AIVs circulating in wild birds in Africa. Presently, there is very limited GenBank coverage (no more than three complete genomes) of non-pathogenic/LP viral genes of AIVs isolated from African wild birds.

Repeated direct transmissions of AIVs from poultry to humans and other mammals have stimulated investigations into the pathogenicity and transmission mechanisms of AIVs in mammals. Prior to the H5N1 'bird flu' incident in Hong Kong in 1997, which marked the first recorded instance of a purely AIV infecting and causing death in humans (Peiris *et al.*, 2007), investigations on the potential of AIVs from waterfowl to infect mammals, including humans, monkeys, pigs, ferrets and cats, have revealed a spectrum of replication, mostly with no significant disease signs (Beare & Webster, 1991; Hinshaw *et al.*, 1981; Kida *et al.*, 1994; Murphy *et al.*, 1982). In recent years, considerable advances have been made in elucidating the determinants of pathogenicity and adaptation of AIVs in mammals, especially for HP isolates involved in human infections (de Wit *et al.*, 2008). However, the mechanisms of pathogenicity and replicative capacity of LPAIVs isolated from wild birds in mammals are still poorly understood.

Sub-Saharan Africa where Zambia is located supports large populations of indigenous waterfowl and is an overwintering area for some Eurasian birds (Olsen *et al.*, 2006). Hitherto, no cases of H5N1 HPAIV have been recorded in southern Africa. Thus, AIV surveillance in wild birds and poultry in this region could provide timely information on the possible introduction of H5N1 HPAIV for mitigation purposes. Additionally, data obtained on LPAIVs in wild birds would expand our current understanding of the ecology and epidemiology of AIVs in this region.

During AIV surveillance conducted between 2008 and 2009 in Zambia, 12 viruses were isolated from wild waterfowl in Lochinvar National Park. Whole-genome sequencing was performed on each isolate, and bioinformatics approaches were employed to characterize the viruses genetically. Furthermore, based on genetic characterization results, we evaluated the replication and pathogenicity of some of the isolates in a mouse model.

RESULTS

Surveillance and virus isolation

AIV surveillance has been ongoing in Zambia since 2006 (Simulundu *et al.*, 2009). Between April 2008 and November 2009, a total of 3094 wild waterfowl faecal specimens were collected in Lochinvar National Park. On average, about 200 faecal specimens were collected every month except during the rainy season (December to March) when the wetland becomes inaccessible due to extreme flooding. Twelve AIVs were isolated (Table 1). Of the 12 isolates, seven were from ducks, four from geese and one from a great white pelican (*Pelecanus onocrotalus*). We identified five different HA (H3, H4, H6, H9 and H11) and NA (N1, N2, N6, N8 and N9) subtypes (Table 1). Among these subtypes, the H11N9 subtype is relatively uncommon, whilst H9N1 is a rare HA/NA combination. Currently, only ten H9N1 isolates are available in GenBank and none has been reported from Africa or Europe.

Phylogenetic analysis of the HA and NA genes

To understand the evolutionary relationships of AIVs isolated from wild birds in Zambia in detail, we sequenced the entire genome of each isolate and conducted phylogenetic analyses. To include, as much as possible, some AIV sequences of isolates from African birds in our analyses, some partial sequences were used. The HA and NA genes of all the viruses characterized in this study belonged to the Eurasian avian lineage (Figs 1 and 2 and Supplementary Figs S1 and S2, available in JGV Online). They clustered mostly with those of AIVs isolated in southern Africa. It was noted that the HA and NA genes of H11N9 viruses reported here formed a distinct sublineage within the Eurasian lineage (see Supplementary Figs S1c and S2c). In this report, only the H6 and H9 HA and the N2 and N8 NA gene trees are described in more detail, because these subtypes have been involved in avian influenza outbreaks in southern Africa.

The topology of the H6 HA phylogenetic tree conformed to that described previously by Bahl *et al.* (2009), particularly in the classification of isolates into the American and

Table 1. AIVs isolated from wild waterfowl in Zambia (2006–2009)

Host	Strain name	Abbreviation	Sampling date
Wild duck	A/duck/Zambia/02/08 (H6N2)	Zb02 (H6N2)	June 2008
	A/duck/Zambia/03/08 (H6N2)	Zb03 (H6N2)	June 2008
	A/duck/Zambia/04/08 (H3N8)	Zb04 (H3N8)	June 2008
	A/duck/Zambia/08/09 (H6N2)	Zb08 (H6N2)	August 2009
	A/duck/Zambia/10/09 (H6N2)	Zb10 (H6N2)	September 2009
	A/duck/Zambia/11/09 (H11N9)	Zb11 (H11N9)	September 2009
	A/duck/Zambia/12/09 (H11N9)	Zb12 (H11N9)	September 2009
Wild goose	A/goose/Zambia/05/08 (H3N8)	Zb05 (H3N8)	July 2008
	A/goose/Zambia/06/08 (H3N8)	Zb06 (H3N8)	July 2008
	A/goose/Zambia/07/08 (H4N6)	Zb07 (H4N6)	September 2008
	A/goose/Zambia/09/09 (H11N9)	Zb09 (H11N9)	September 2009
Wild pelican	A/pelican/Zambia/01/06 (H3N6)*	Zb01 (H3N6)	August 2006
	A/pelican/Zambia/13/09 (H9N1)	Zb13 (H9N1)	November 2009

*The first influenza virus isolate from an avian host in Zambia (Simulundu *et al.*, 2009).

Eurasian/American lineages (Fig. 1a). The H6 HA genes reported in this study belonged to a group of viruses of the Eurasian/American lineage that consisted of contemporary H6 strains isolated from wild aquatic birds in Africa, Asia and America, including those viruses that were introduced into terrestrial poultry in Taiwan and South Africa (Fig. 1a). They shared a common ancestor with an H6N8 virus that caused avian influenza in South African ostriches in 2007 (Abolnik *et al.*, 2010) (Fig. 1a). The H6 HA genes of the isolates obtained in Zambia were distinct from those that caused an avian influenza outbreak in chickens in South Africa in 2002.

Genetic and antigenic analyses of the HA genes of H9N2 AIVs have shown that these viruses separate into three main Eurasian lineages (Xu *et al.*, 2007). These lineages are represented by chicken/Beijing/1/94, quail/Hong Kong/G1/97 and duck/Hong Kong/Y439/97 (Fig. 1b). The HA gene of Zb13 (H9N1) belonged to the duck/Hong Kong/Y439/97-like lineage (also called the Korean lineage) and was most closely related to that of ostrich/South Africa/AI1586/08 (H9N2).

In the N2 NA gene tree, AIVs isolated in this study fell in a Eurasian sublineage composed of viruses isolated mainly from wild aquatic birds in Asia, Europe and Africa (Fig. 2a). They clustered together with strains isolated from an ostrich and from a wild goose in South Africa in 2008, as well as two other strains isolated in China and Japan. The H5N2 AIVs with a genotype characteristic of HPAIVs detected from wild ducks in Nigeria also belonged to this sublineage. The N2 NA phylogeny further revealed that the N2 genes of viruses that caused outbreaks of avian influenza in South Africa in 2002 were distinct from those characterized in this study, a finding that is in concordance with their HA phylogenetic comparisons (Figs 1a and 2a).

Phylogenetic analysis of the N8 NA genes showed several sublineages within the Eurasian avian lineage, namely, early 1 and 2, contemporary 1 and 2 and European gull isolates (Fig. 2b). The NA genes of Zb04 (H3N8), Zb05 (H3N8) and Zb06 (H3N8) belonged to the contemporary 1 sublineage, which consisted of AIVs isolated mostly from wild birds in Europe and southern Africa.

Phylogenetic analysis of the internal protein genes

Broadly, the topologies of the internal protein gene trees showed assortment of the AIVs into the American and Eurasian avian lineages, with early and contemporary sublineages being identifiable in the latter lineage, as described previously by Duan *et al.* (2007). The Eurasian contemporary sublineage was further divided into two to three groups.

Phylogenetic analysis of the PB2 polymerase subunit gene showed that, except for Zb04 (H3N8) which fell in group 2 of the Eurasian contemporary sublineage, all the viruses isolated in Zambia from 2006 to 2009 clustered together in group 1 (Fig. 3a). H5N1 HPAIVs also joined this group, but they were not closely related to the viruses reported here. The PB2 gene of Zb04 (H3N8) showed a close relationship to those of two H5N2 viruses isolated from domestic ducks in China.

In the PB1 polymerase subunit gene tree, three groups were observed in the Eurasian contemporary sublineage (Fig. 3b). All isolates from waterfowl in Zambia belonged to group 3. Whilst the majority of the strains isolated between 2006 and 2009 in Zambia grouped together as an independent branch, the PB1 genes of Zb04 (H3N8), Zb08 (H6N2), Zb10 (H6N2) and Zb13 (H9N1) belonged to a cluster of viruses that included two recent wild-bird isolates from South Africa, two H5N2 influenza viruses isolated from pigs in South Korea and two H5N1 HPAIVs isolated in Laos (Fig. 3b).

In the PA polymerase subunit phylogeny, all the viruses reported here belonged to group 1 and the majority of the

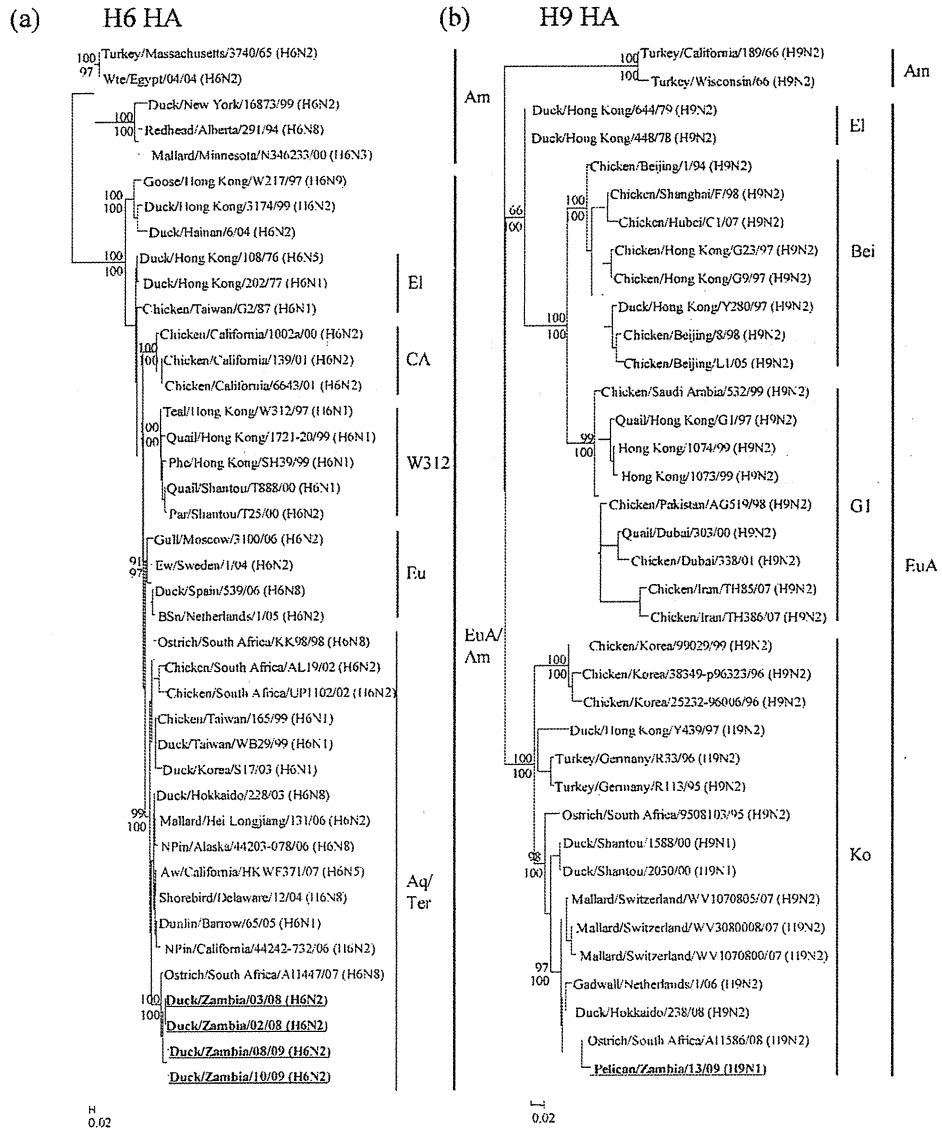

Fig. 1. Phylogenetic relationships of the H6 HA (a) and H9 HA (b) genes of AIVs isolated from wild birds in Zambia. Analysis was based on nt 44–1066 (1023 bp) of H6 HA and 97–1228 (1132 bp) of H9 HA. Numbers above and below branch nodes indicate neighbour-joining bootstrap values of ⩾50 % and Bayesian posterior probabilities of >95 %, respectively. Owing to space limitations, not all supports are indicated. Virus strains characterized in the present study are bold and underlined. Bars, number of substitutions per site. Lineages: Am, American; Aq/Ter, aquatic/terrestrial; Bei, chicken/Beijing/1/94-like; CA, California; El, early; Eu, Europe; EuA, Eurasian; G1, quail/Hong Kong/G1/97-like; Ko, Korean-like; W312, teal/Hong Kong/W312-like. Strain names: Aw, American wigeon; BSn, Bewick's swan; Ew, Eurasian wigeon; NPin, northern pintail; Par, partridge; Phe, pheasant; Wte, whiskered tern.

viruses grouped with those of AIVs isolated from wild birds and ostriches in South Africa (Fig. 3c). The PA gene of Zb04 (H3N8) showed a close relationship to viruses isolated from wild birds in the Netherlands. The PA gene of Zb01 (H3N6) belonged to group 2 and clustered with those of the Asian H5N1 HPAIVs, as we reported previously (Simulundu *et al.*, 2009).

The nucleoprotein (NP) gene tree showed the division of the Eurasian contemporary sublineage into three groups (Fig. 4a). All the viruses characterized in this study assorted to group 3. Eight of these strains, along with those isolated recently from wild and domestic birds in South Africa, formed a distinct cluster within this sublineage. The other four isolates clustered with viruses isolated mostly from